Lichen Detectibility under Varying Canopy Closure

By:
Nicole Robichaud

Faculty of Natural Resources Management
Lakehead University
Thunder Bay, Ontario

LICHEN DETECTIBILITY UNDER VARYING CANOPY CLOSURE

by

Nicole Robichaud

An Undergraduate Thesis Submitted in Partial Fulfillment of the Requirements for the Degree of Honours Bachelor of Science in Forestry

Faculty of Natural Resources Management

Lakehead University

April 2019

Ashley Thomson	Alex Bilyk
________________________	________________________
Thesis Supervisor	Second Reader

LIBRARY RIGHTS STATEMENT

Signature:______________________________

Date: 04/24/2019

A CAUTION TO THE READER

This HBScF thesis has been through a semi-formal process of review and comment by at least two faculty members. It is made available for loan by the Faculty of Natural Resources Management for the purpose of advancing the practice of professional and scientific forestry.

The reader should be aware that opinions and conclusions expressed in this document are those of the student and do not necessarily reflect the opinions of the thesis supervisor, the faculty or Lakehead University.

ABSTRACT

Robichaud, N.D. 2019. Lichen detectability under varying canopy closure. 55pp.

Keywords: boreal forest, caribou, Dryden, lichen, Near Infrared (NIR), Normalized-Difference Vegetation Index (NDVI), unmanned aerial vehicle (UAV), Visible-Band Difference Vegetation Index (VDVI).

Monitoring lichen distribution is of increasing concern as mapping is critical in characterizing habitat for woodland caribou. Aerial photography collected using drones, the method used for this study, is a common method of lichen detection and is usually paired with field data collection. It employs cameras that provide images with red green blue (RGB) and near-infrared (NIR) bands. Low accuracies obtained from aerial drone imagery have been attributed to stand and site features restricting accurate readings. Thus, before lichen mapping can be utilized on a broad scale, it is important to identify the amount of canopy closure under which classification accuracy is negatively affected. This was determined by classifying seven sites with varying canopy closure, resulting in classification accuracies corresponding to each plot. This report provides a current analysis of lichen detection under varying canopy closure. The objective of this study is to determine the crown closure percentage, as calculated by the winSCANOPY program, and its effect on lichen detection using drone imagery. The study was conducted in Dryden, Ontario, where the correlation between canopy closure and lichen detection was made. It was found that below 88% canopy closure, lichen classification accuracy significantly decreases and below 77% canopy closure, overall image classification is affected. The findings in this study support the hypothesis that canopy closure is directly correlated to the classification efficiency of UAV imagery, however further investigation into improving classification is required. Further investigation into the effects of bare ground and rock outcrop misclassification should also be conducted, as this played a significant role in lichen classification.

CONTENTS

TABLES

FIGURES

ACKNOWLEDGEMENTS

I would like to acknowledge my thesis advisor Dr. Ashley Thomson and my second reader Alex Bilyk for their invaluable input in shaping my thesis. I would like to thank Ryan Wilkie for providing advice and data pertaining to the data analysis portion of this thesis. I would also like to thank Robert Glover for participating in the data collection portion of this thesis. Finally, I would like to give an extended thanks to Frank Luckai, who provided insight, encouragement and support throughout this analysis. His knowledge of winSCANOPY software served invaluable in ensuring my data analysis was completed.

INTRODUCTION

The reindeer lichen (*Cladonia rangiferina* (L.) F. H. Wigg.) is a fructicose ground lichen that occurs in boreal pine forests and open, low-alpine sites in a wide range of habitats from humid, open forests, to rocks and heaths. As the name suggests, it is an important food for woodland caribou (*Rangifer tarandus caribou*), a threatened species, having great ecological importance as a result. Monitoring lichen distribution is therefore of increasing concern as mapping lichen distribution is critical in characterizing habitat for woodland caribou (Gilichinsky et al. 2011).

Studies have been carried out using multiple technologies to identify reflectance characteristics of different ground lichen species. Reindeer lichen have a strong absorption of ultraviolet, blue and yellow wavelengths (Petzold and Goward 1988; Rees et al. 2004; Nelson et al. 2013), with a high influence of view and sun angles (Solheim et al. 2000). Bioactive compounds found within reindeer lichen with exposure to ultra violet B (UV-B) radiation induces the accumulation of usnic acid and melanic compounds, which is found to have a spectral signature. The reflectance from blue wavelengths are significant in *Cladonia* lichen responses however, the spectral distinction of usnic acid in this lichen increase accuracy in detecting yellow pigments, allowing for better classification results (Peltoniemi et al. 2005; Nelson et al. 2013).

Satellite remote sensing has facilitated the determination of vegetation richness and cover distribution and has great potential for areas with limited access. Most studies considering lichen detection are based on the analysis of the Normalized Difference Vegetation Index (NDVI) (Jarcuska et al. 2010). NDVI has been used to indicate the presence of chlorophyll in an image, detecting visible red light and near-infrared (NIR) (Nelson et al. 2013). Aerial photography collected using drones is a common method of lichen detection and is usually paired with field data collection. Aerial and LiDAR imagery has resulted in varying resulting accuracy; however, all have fallen at an average below 70% (Waser et al. 2007; Waser et al. 2004; Korpela 2008). These low accuracies from aerial drone imagery are thought to correlate to canopy-condition restricting accurate readings.

Under a canopy, the understory is in direct light, shade, or full shadow, and in optical remote sensing the reflected signal from the understory is mixed with that from the upper canopy, which may complicate the interpretation of images (Korpela 2008). It is therefore difficult to separate understory species using satellite images, limiting detection of understory species through canopy closure. Many types of equipment have been employed in studies aimed at detecting the occurrence of lichen using remote sensing technologies such as Landsat data, hyperspectral image scanner data, aerial photographs, and LiDAR. Aerial photography collected using drones is a common method of lichen detection that usually employs cameras that provide images with red green blue (RGB) and NIR bands (Waser et al. 2007; Waser et al. 2004). Literature suggests low accuracies obtained from aerial drone imagery have been attributed to canopy-closure restricting accurate readings (Rautiainenetal et al. 2007; Korpela 2008). Thus, before lichen mapping can be widely utilized, it is important to identify the amount of canopy closure under which accurate detection is affected.

WinSCANOPY is a digital image analyser for canopy and solar radiation analysis that measures leaf area index (LAI), canopy openness, site factors, NDVI, and other characteristics of the crown (Jarcuska et al. 2010). The images taken using this technology are hemispherical, allowing for the classification of canopy cover and sky. The system can be used in a laboratory, at remote locations, or in the field on portable computers (Murray 2013). This technology is therefore expected to have potential for determining the range of percent canopy-closure under which lichen detection is possible.

This report provides a current analysis of lichen detection under varying canopy closure. It will serve to delineate the amount of crown closure that significantly reduces image classification accuracy. This study is important as classification accuracy is vital for the application of lichen detection using aerial imagery for management purposes. The objective of this study is to determine the crown closure percentage, as calculated by the winSCANOPY program, and its effect on lichen detection using drone imagery. Plots used for the purpose of this study were in Dryden, Ontario, allowing for the correlation between canopy closure and lichen detection in a Boreal forest landscape.

LITERATURE REVIEW

REMOTE SENSING OF LICHEN COVER IN FORESTED ENVIRONMENTS

Lichen detection through variable forest canopy cover using remote sensing techniques is a practice that is faced with numerous challenges in technology and accuracy. These challenges include classification accuracy and precision, limited camera qualities and environmental constraints. A large body of scientific research has been aimed at developing new remote sensing tools and processing software (Falldorf et al. 2014; Theay et al. 2004; Nordberg and Allard 2002; Murray 2013). Therefore, it is important to consider the various possible uses of available equipment, the processing software used to build images and detection platforms, the methodology of collecting data, and the applicability of a digital image analyser for canopy and solar radiation analysis within this research.

Many types of equipment have been employed in studies aimed at detecting the occurrence of lichen using remote sensing technologies (Faldorf et al. 2014; Theau and Deguay 2004; Faldoff et al. 2013; Theau and Duguay 2004; Nordberg and Allard 2002; Korpela 2008; Waser et al. 2007). The various imagery types that have been used include Landsat data (Faldorf et al. 2014), hyperspectral image scanner data (Nordberg and Allard 2002), aerial photographs (Waser et al. 2007) and LiDAR (Korpela 2008). Falldorf et al. (2014) determined that bands 2, 4, and 5 of Landsat imagery provided improved results in lichen detection when compared to other bands. A modest correlation between the normalized difference lichen index (NDLI) and lichen volume was found with the strongest sensitivity at intermediate lichen cover but poorer estimates were obtained at low and high volumes of lichen (Theau and Duguay 2004; Faldorf et al.

2013). Theau and Duguay (2004) found that radiometrically normalized Landsat thematic mapper images have high utility for monitoring lichen cover over large, remote areas, returning 80 to 90% accuracy. A validation test run during this study displayed a good linear relation between lichen fraction estimated in the field and that obtained with the spectral mixture analysis (SMA) procedure developed by Theau and Duguay (2004). SMA is a sub-pixel classification technique, depending on spectral response of land cover components (Theau and Duguay 2004). Nordberg and Allard (2002) found that the camera position, atmospheric interference (e.g. cloud cover), and seasonal timing (i.e. varying phenological states between image dates) influenced the effectiveness of multi-temporal satellite image data for lichen change detection. As presented by Korpela (2008), LiDAR held similar potential for lichen detection when compared to Landsat images. Lichen surfaces had a higher NIR value where normalization of intensities allowed for increased seperability of lichens from other surfaces, thereby improving accuracy. Nordberg and Allard (2002) assessed hyperspectral imaging scanner data as another lichen detection technology. However, hyperspectral imaging proved ineffective for use with lichen detection as the instrument response was too low in the middle infrared (MIR) part of the spectrum. Airborne digital color infrared (CIR) ortho-images were used in a study by Waser et al. (2007), combining multispectral bands with Quickbird satellite data. Using airborne remote sensing data proved moderately effective, with 45% accuracy as demonstrated by Waser et al. (2004).

PROCESSING METHODS USING LANDSAT FOR LICHEN DETECTION

Several different methods used to detect lichen cover based on Landsat imagery differ in their effectiveness (Falldorf et al. 2014; Rees et al. 2004; Neta et al. 2010; Nordberg and Allard 2002). Normalized difference moisture index (NDMI) is a processing method that contrasts NIR, a band that is sensitive to the reflectance of leaf chlorophyll content, to the MIR band, which is sensitive to the absorption of leaf moisture. This method was utilized by Falldorf et al. (2014) resulting in successful identification on various lichen volume classes. Rees et al. (2004) demonstrated that lichens of the species *Cladonia, Stereocaulon,* and *Flavocetraria* are easily separated from each other using MIR, and Neta et al. (2010) demonstrated that this technology is also effective for detecting wet lichen. Falldorf et al. (2014) further displayed the utility of a lichen volume estimator (LVE) which was developed using remote sensing and field measurements. A Landsat TM land cover mask was used to separate lichen heath communities from other vegetation types and lichen volume was estimated, resulting in an average accuracy of 67% (Falldorf et al. 2014). This model can be a valuable tool to predict quality of pastures for reindeer and caribou. It also performs better than any other prediction model developed for quantifying lichen abundance. Falldorf et al. (2014) used orthorectified United States Geological Survey (USGS) images, processed using ERDAS Imagine based on a digital elevation model (DEM) and ground control points, and concluded that NDMI and NDLI both function in identifying lichen volume. These models, however, returned much lower accuracies than the LVE, with 61% and 37% accuracy, respectively. Furthermore, NDLI was significantly less effective for volume classes below $60m^3/m^3$. Promising results were shown by Nordberg and Allard (2002) for vegetation-index differencing as a means of lichen change detection using Landsat Thematic Mapper (TM) data, especially when using NIR wavelengths, resulting in a mean overall accuracy of 85%. A study conducted by Theau and Duguay (2004) used the classification procedure named the enhancement-classification method (ECM), which operated on three input channels and produces a classification in which all relevant spectral content is extracted. The suitability of ECMs and an SMA to identify lichen land cover over large areas was then analysed. The ECM and SMA methods are appropriate for different aspects of lichen mapping. The ECM method provides good discrimination between lichen and non-lichen classes resulting in an overall classification accuracy of 83.9%. Conversely, SMA provides additional lichen information not available from classification but important for environmental application. The SMA procedure resulted in 79.7% of lichen sites being accurately selected. For this reason, Theau and Duguay (2004) recommended to use a combination of both SMA and ECM for future research. The use of a matched filtering algorithm, which partially unmixes images to aid in detection of a given material, performed by Casanovas et al. (2015) allowed for lichen detection using MIR satellite imagery. The matched filtering failed to detect the presence of lichens in only 7% of the sites studied, whereas the NDVI failed to detect 47% of lichen on the site. Therefore, a significant improvement in accuracy was observed when using this algorithm. Another processing method included using spectral bands when running analysis. Nelson et al. (2013) utilized this method where a regression against spectral and environmental predictor variables with non-parametric multiplicative regression (NPMR) in the program HyperNiche was run where lichen with usnic, an acid with a pale-yellow pigment found in most lichen caribou eat, increased accuracy by 31% as it is spectrally distinct.

AERIAL PHOTOPGRAPHY FOR LICHEN DETECTION

Aerial photography collecting using drones is a common method of lichen detection and is usually paired with field data collection. Using cameras that provide images with RGB and NIR bands is a standardized method of airborne lichen detection

(Wilkie 2018; Waser et al. 2007; Waser et al. 2004), where various processing methods may then be applied. Waser et al. (2004) reported 48% accuracy for detecting ground lichen using aerial photography. Wilkie (2018) reported higher accuracies, averaging 68%. Low accuracies from aerial drone imagery, as discussed by Wilkie (2018) and Waser et al. (2004), may be due to canopy-closure restricting accurate readings. Korpela (2008) concurred with this finding, discussing the reduced accuracy that was experienced using airborne LiDAR data under high canopy-closure. The large-scale aerial images utilized by Korpela (2008) were taken using a Vexcel UltraCam D digital camera which is a multi-lens, multispectral, two-resolution frame sensor. This resulted in 65-75% accuracy, an insufficient accuracy for most monitoring applications. Identifying the amount of canopy closure that impedes accuracy in lichen detection is therefore crucial if wanting to apply these methods to management programs.

LIMITATIONS DUE TO CANOPY COVER SURROUNDING LICHEN DETECTION

Under a canopy, the understory is in direct light, shade, or full shadow, and in optical remote sensing the reflected signal from the understory is mixed with that from the upper canopy, which may complicate the interpretation of images (Korpela 2008). Korpela (2008) concluded that LiDAR is particularly effective in its ability to map topographic relief under forested conditions, as it provides a means of finding gaps in the canopy, where the understory flora, such as lichen, can be sampled without interruption from canopy closure. It is an active instrument which remains largely unaffected by the occurrence of forest canopy. Using simulations with a forest reflectance model, Rautiainenetal et al. (2007) concluded that the distribution of the understory to total nadir reflectance had a broad range, depending on canopy cover. These results suggest that the separation of understory species using satellite images may be possible using visible bands of satellite images in thin canopies.

USING A DIGITAL ELEVATION MODEL LAYER TO IMPROVE ACCURACY

A DEM is an array of regularly spaced elevation values that are referenced to a Universal Transverse Mercator (UTM) projection or to a geographic coordinate system (Li and Chen 2005). The addition of a DEM layer to improve accuracy has been explored by a multitude of authors, allowing for another vector to improve precision (Franklin et al. 1991; Franklin 1994; Nagendra 2001). Franklin et al. (1991) used a Compact Airborne Spectrographic Imager (CASI), a hyper-spectral sensor, where classification improved from 81% to 90% when a DEM was incorporated into the analysis. In a similar study by Franklin (1994), using the Système Pour l'Observation de la Terre (SPOT) and Landsat TM data, accuracy was improved by 11% with the addition of a DEM layer into the classification scheme. Therefore, it has been found that the addition of a DEM layer into classifications has the potential to significantly improve accuracy, especially when considering shrub and bare ground (Nagendra 2001; Franklin et al. 1991; Franklin 1994).

WINSCANOPY AS A TOOL FOR CALCULATING CANOPY CLOSURE

WinSCANOPY is a digital image analyser for canopy and solar radiation analysis measuring LAI, gap fraction, canopy openness, site factors, NDVI, and other factors (Jarcuska et al. 2010). Jarcuska et al. (2010) and Murray (2013) utilized winSCANOPY technology for calculating accuracy for relative diffuse and relative direct transmittance, canopy openness, and LAI, where pixel classification was the main method applied. Jarcuska et al. (2010) used a Nikon P5000 digital camera and Nikon FC-E8 fisheye lens converter with 183˚ view angle from Régent winSCANOPY accessories. Jarcuska et al (2010) examined the utility of winSCANOPY in pixel classification when analysing hemispherical images. It was determined that the technology functions well in identifying diffuse under-canopy radiation and leaf area index. Murray (2013) used winSCANOPY to assess availability of light to herb-layer vegetation with similar results. A pixel classification based on grey scale was used for processing, allowing for effective identification of diffuse under-canopy radiation and LAI. The images taken using this technology were hemispherical, allowing for the classification of canopy cover and sky. This technology is therefore postulated to have potential to be used for determining the range of percent canopy-closure under which lichen detection is possible. However, there have been no studies to date that have examined the effectiveness of winSCANOPY for the previously mentioned purpose.

THE IMPORTANCE OF MONITORING LICHEN

Ground lichens that are a preferred food source for woodland caribou (*Rangifer tarandus caribou*) and various studies on this species of lichen have been conducted in remote sensing literature (Petzold and Goward 1988; Colpaert et al. 1995; Arseneault et al. 1997; Nordberg and Allard 2002; Rees et al. 2003; Gilichinsky et al. 2011). Most reindeer lichen classification studies have focused on methods of pixel-wise supervised classification and have produced thematic classes of lichen cover (Petzold and Goward 1988; Colpaert et al. 1995; Arseneault et al. 1997). Recent studies have put greater emphasis on integrating remote-sensing data and ancillary forest cover data for mapping ground lichens for future application in management and monitoring (Nordberg and Allard 2002; Rees et al. 2003; Gilichinsky et al. 2011). Monitoring lichen distribution is of increasing concern due to increased soil temperatures in northern latitudes, leading to tree and shrub expansion, as concluded by Nelson et al. (2013). The need for new tools for measuring large-scale woody plant encroachment is discussed, as such tools would allow for the detection of changes in foraging resources (Nelson et al. 2013). Gilichinsky et al. (2011) discusses how lichen distribution is critical for characterising habitat for woodland caribou, a threatened species.

LICHEN DETECTION

Studies have been carried out using multiple technologies to identify reflectance characteristics of different ground lichen species (Petzold and Goward 1988; Solheim et al. 2000; Rapalee et al. 2001; Solheim et al. 2000; Peltoniemi et al. 2005; Nelson et al. 2013). Using a radiometer and spectrometer, Petzold and Goward (1988) found that *Cladina* lichen had a strong absorption of ultraviolet and blue wavelengths. Rees et al. (2004) used a spectroradiometer to study species reflectance of various lichen samples from subarctic tundra habitats in northern Sweden, finding no reflectance peak in the green wavelength. Solheim et al. (2000) measured spectral properties of *Cladina* lichens and moss using a goniospectrometer, concluding lichen reflectance varied significantly according to view and sun-angles. It was determined by Peltoniemi et al. (2005) that *Cladina* lichens display strong backscattering and are distinct from other vegetation and soil. These studies have suggested that reflectance from blue wavelengths are significant in *Cladina* lichen spectral responses. Rapalee et al. (2001) found, using Landsat TM and Advanced Very High-Resolution Radiometer (AVHRR) data, that ground cover, overstory composition, and density were significant predictor variables in determining accuracy of classified lichen. Nelson et al. (2013) concluded that *Cladonia* lichen are lighter colored, reflecting more light in blue to yellow wavelengths when compared to green vegetation. Although no study has focused on the continuous mapping of usnic lichen, Nelson et al. (2013) discussed that usnic lichen is in most lichen that caribou eat, having a pale-yellow pigment. This renders the lichen spectrally distinct which is a useful characteristic in remote sensing.

MATERIALS AND METHODS

MAPPING AND IMAGE COLLECTION

The imagery used in this report was collected by the NCASI caribou project team as a part of a study to examine the potential for lichen detection using drone imagery as outlined in Wilkie (2018). Briefly, aerial images were obtained for seven plots near the town of Dryden, Ontario (Figures 1 and 2) using a DJI Inspire 1 drone equipped with two sensors (stock X3 RGB colour camera and a modified X3 camera capable of capturing NIR) at 90 m elevation. Images of crown closure were obtained using a winSCANOPY unit outfitted with a fisheye lens to capture plot centre images looking upward.

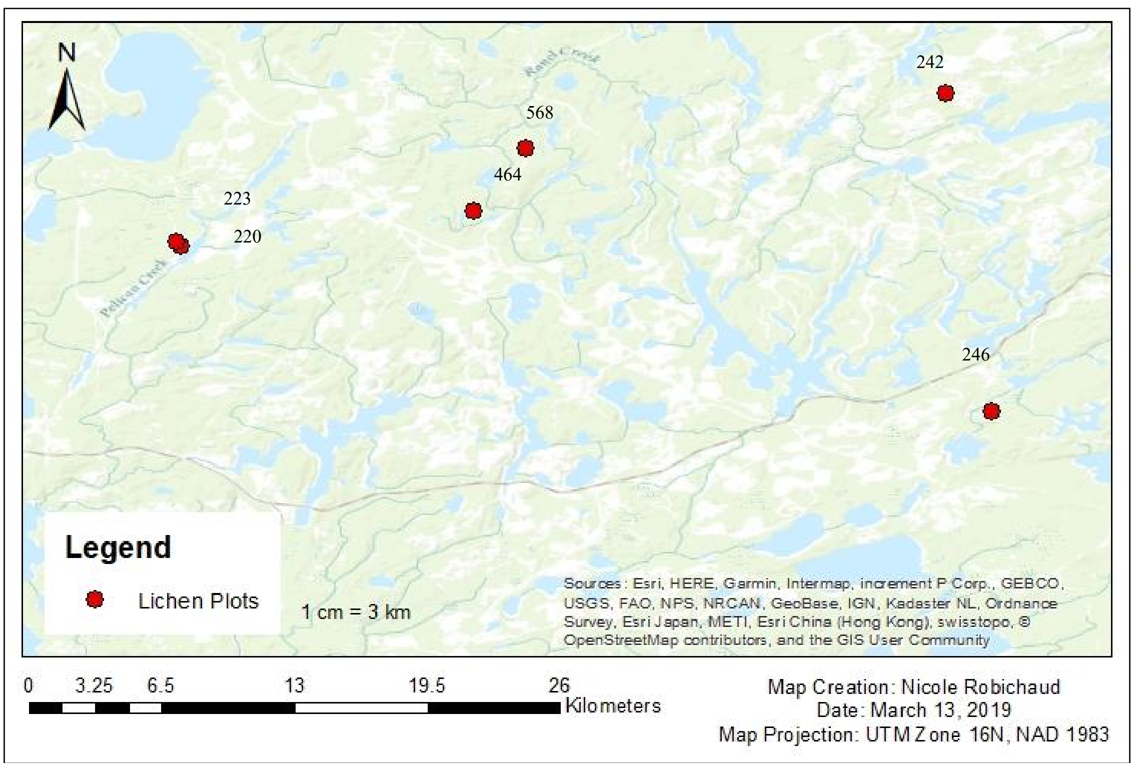

Figure 1. Location of six plots visited in Dryden, Ontario

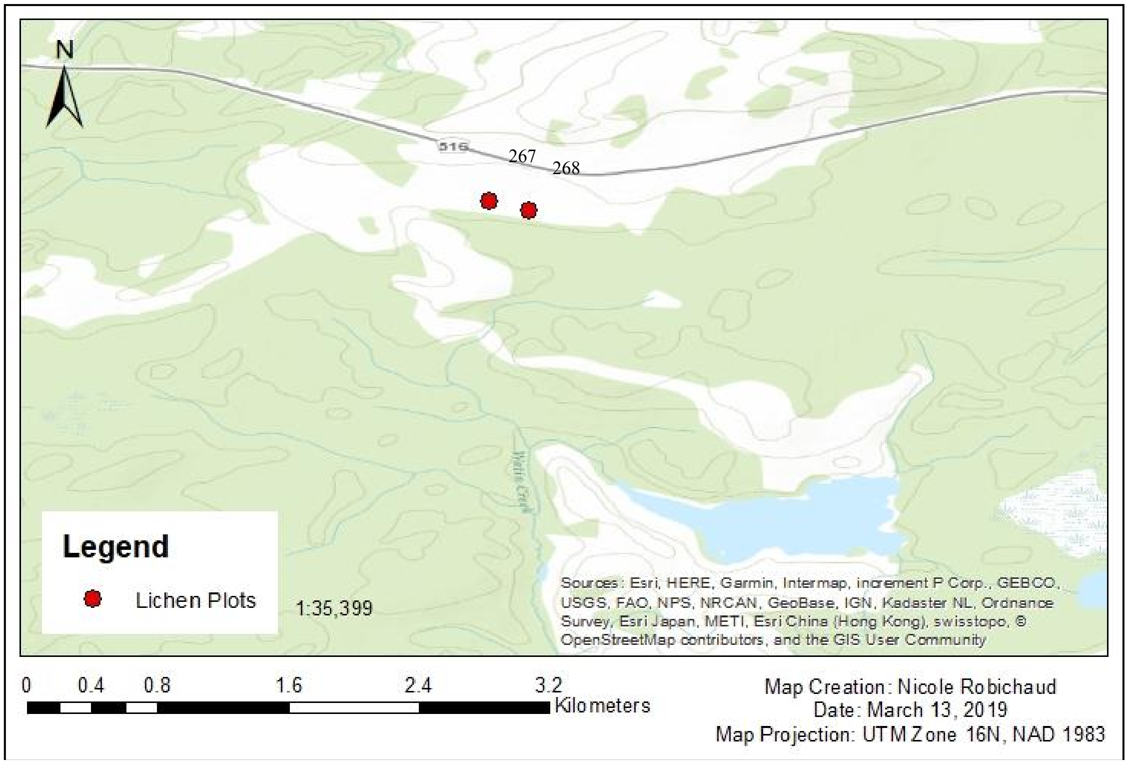

Figure 2. Location of plots 267 and 268 visited in Dryden, Ontario

DATA PROCESSING

The NIR and RGB layers of each flight were stacked along with the DEM layer, resulting in seven images to be classified. Sites 267 and 268 fell under the lichen “stand” type one, sites 242 and 568 fall under type two, 246 and 464 are type three, while 220, 223, and 568 again are type four (Appendix I). Images were then classified to extract features such as lichen in eCognition. Classifications were then exported as shapefiles where accuracy assessments could be done on each site. Accuracy assessments could then be reviewed to compare the classification rules and if lichen extents can be extracted from unmanned aerial imagery.

Image data provided by the NCASI team were organized by site number, sensor type (RGB or NIR) and flight elevation (Wilkie 2018). The NIR camera captures three bands, therefore the NIR bands were added to the RGB image file in eCognition. In the *Modify open project* tab, layers were reduced resulting in five layers in the final processed image, which included a DEM layer. These layers were then used to develop the ruleset that would drive the classification of images, across each site. The goal of classification was to create an automated classifier that could be applied broadly, to many different photos at many different resolutions. Therefore, the rules start with a broad spectral separation into the prospective classes with sequential rules to aid in refining the overall classification. Custom rulesets were developed for each image to then further refine classification accuracy.

Within these classifications, a Visible-Band Difference Vegetation Index (VDVI) was made as a customized arithmetic function presented below (Xiaoqin *et al.* 2015). This layer is commonly used for classifying vegetation.

$$VDVI = \frac{2*[Mean\ Green] - [Mean\ Red] - [Mean\ Blue]}{2*[Mean\ Green] + [Mean\ Red] + [Mean\ Blue]} \qquad \text{Equation (1)}$$

The Normalized Difference Vegetation Index (NDVI) layer was developed for application to UAS imagery and the equation used is presented below;

$$NDVI = \frac{[Mean\ NIR] - [Mean\ Red]}{[Mean\ NIR] + [Mean\ Red]} \qquad \text{Equation (2)}$$

The Vegetation Index (VI) layer was developed for application to RGB imagery to increase vegetation classification accuracy using the below equation (Jiang *et al.* 2008).

$$VI = \frac{2.5\ (Mean\ NIR - Mean\ Red)}{L + Mean\ NIR + C_1\ Mean\ Red - C_2\ Mean\ Blue} \qquad \text{Equation (3)}$$

This equation is for an enhanced vegetation index, where the variable L represents 1, variable C_1 represents 6, and variable C_2 represents 7.5. This layer will improve sensitivity to a wider, global range of vegetation conditions and better depict vegetation canopy structural parameters.

The ruleset for image classification was then built, as can be seen in Figure 3, focusing on using values from the NDVI, VDVI, VI layers, mean layer values, DEM layers, and ratio layer values. The additional rules made for each image was based around the DEM layer and ratio NIR classifications and can found in the Appendices.

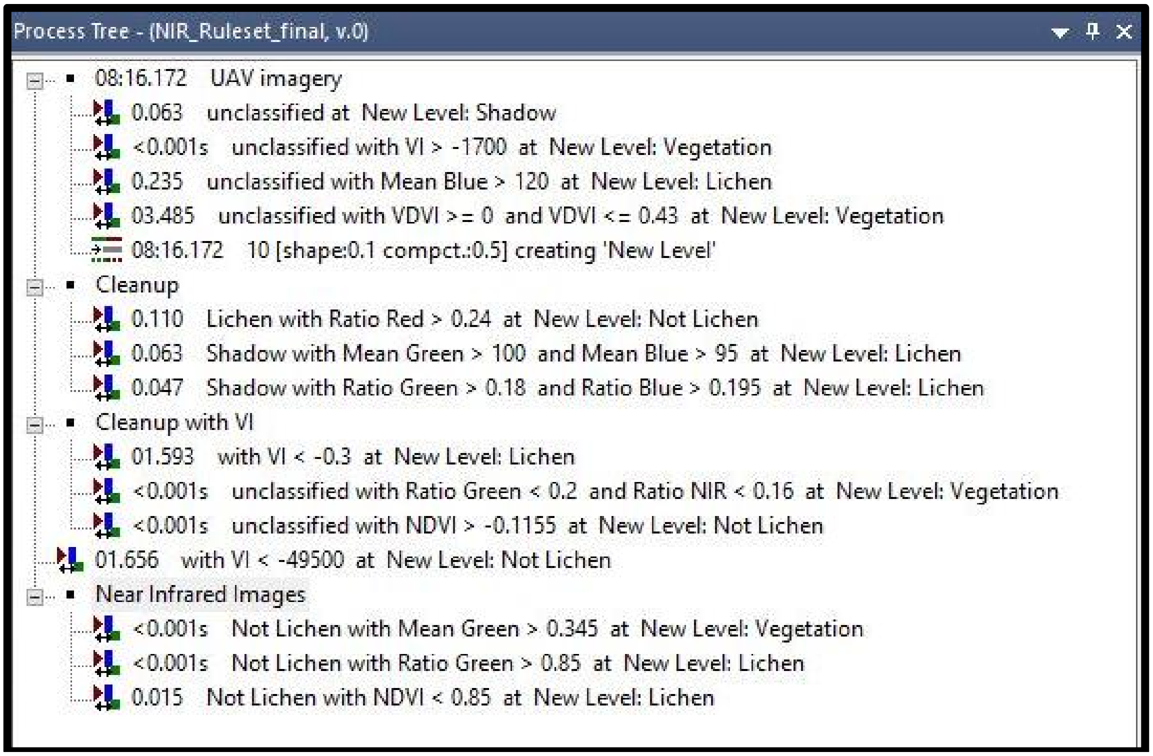

Source: eCognition 2019

Figure 3. Universal ruleset for image classification

Once classification was completed to a satisfactory level, files were exported as shapefiles. All classes were selected for export excluding the ‘unclassified’ class. The features selected include the relations to classification class name and the ‘object features geometry extent area’. Once exported, the classified shapefile was then opened in ArcGIS and clipped to the plot extent.

An excel spreadsheet with two columns, class names and class number, was created. This sheet was used to ensure precision throughout each analysis (Appendix X). Next, the polygon specific to each site was loaded into ArcGIS. For each of the 7 sites, 100 random points were created, where a polygon was used as the constraining feature class. A quality control (QC) image for each site was loaded. For each sample point layer, a new column is added, called reference class. Editing was enabled, and using the QC image, each point was labelled the class it represented on the ground and the classification it was assigned. This process was executed in ArcGIS for each of the seven images.

In ArcGIS, the classified shapefile was loaded. The quality control points, the Excel reference table, and the clipped 4-band image were opened. This resulted in a point layer with class name, term ‘Classification’, and a reference value for each point within the block. Each reference class point was also assigned a ‘Real’ number (1 to 4), signifying what the classification should have been. Once all points had both columns filled out, the table was exported to excel. In excel, the percent accuracy of both image classification and lichen classification was computed. This was done through a binary process, each point being classified as either 1, correctly classified, or 0, being incorrectly classified. These columns were then averaged and multiplied by 100.

Seven photos taken with the winSCANOPY unit were uploaded to eCognition and classified into sky and tree cover using the nearest neighbour method. Once each image was classified, a screen grab of the classified image was saved as a JPEG file, later used in the winSCANOPY program. Each image file was uploaded to the winSCANOPY program and a horizon was built to delineate the border of the circular photo. A grey scale pixel classification was then run, for the program to better understand which areas were sky and which were tree cover. A canopy analysis was then run, providing information on canopy closure, LAI, gap fraction, and other site factors. Screen grabs of each analysis were taken, and image analysis data was saved as TIFF files. The percent canopy closure observed from each plot was recorded onto an excel sheet.

RESULTS

A strong correlation was found between lichen classification accuracy and percent canopy closure. Canopy cover ranged from 6 to 88% while lichen classification accuracy ranged from 30 to 82%. Figure 4 displays one of the classified images, plot 242**,** which was put into ArcGIS to undergo an accuracy assessment, resulting in a classification accuracy. The red areas in the image represent the lichen feature class, the blue represents not lichen, the green is the classified vegetation feature class, and the black represents shadows. This plot classified lichen with 82% accuracy and had an overall pixel-based accuracy of 86%.

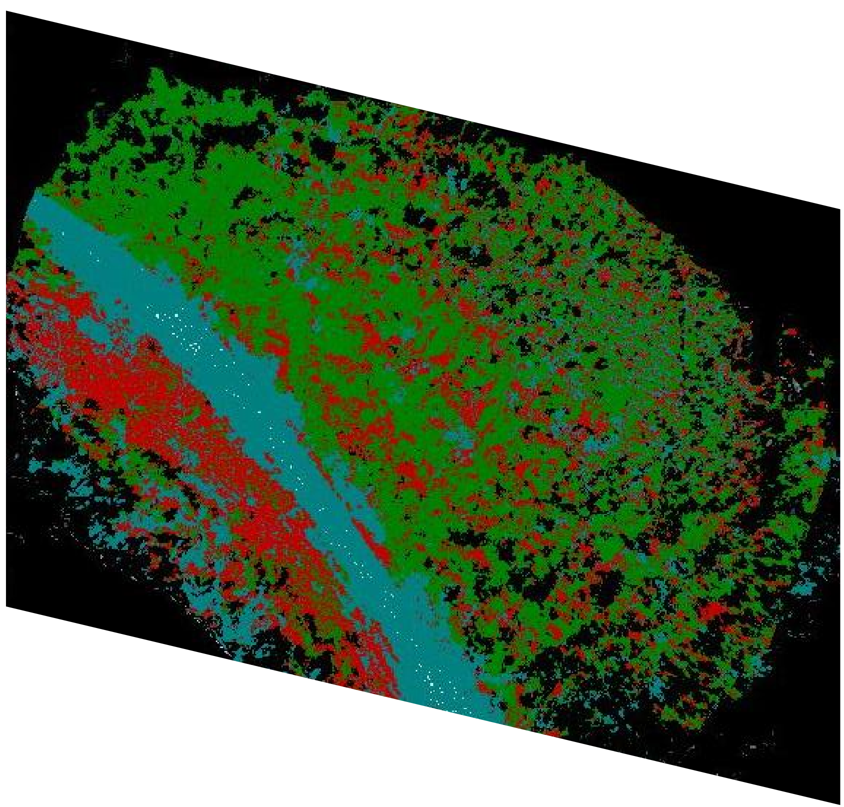

Source: eCognition 2019

Figure 4. Classified image of Plot 242

Figure 5 displays an image that has been analyzed using winSCANOPY, after being classified in eCognition. The left margin displays global data, site factors, and various other light values. Within this column, openness is listed, which is the value used for the percent of canopy closure. This image displays site 267 which had 49% canopy closure.

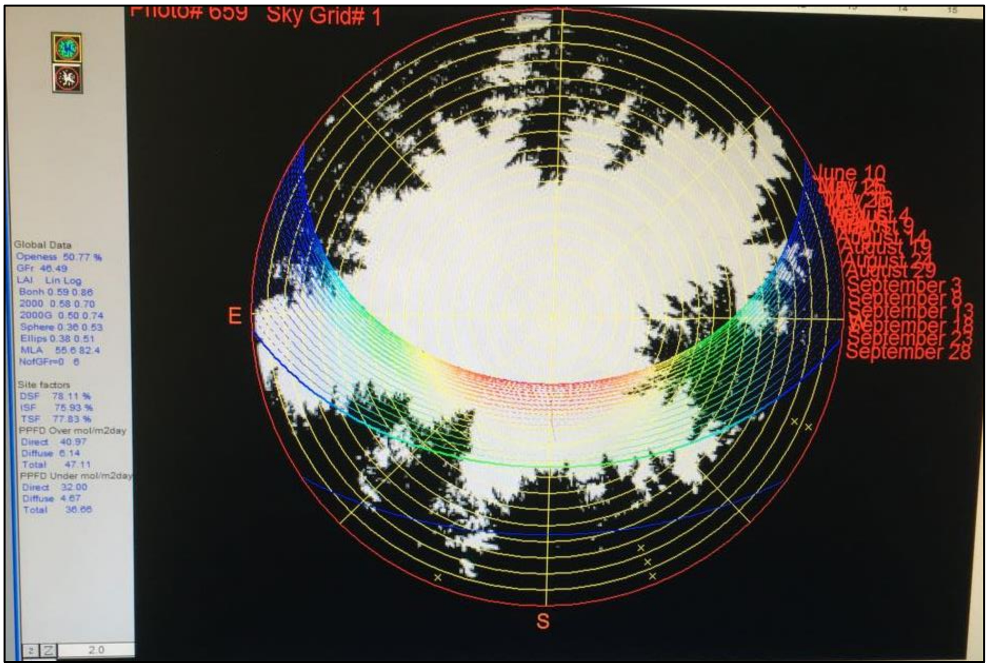

Source: WinSCANOPY 2018

Figure 5. Plot 267 WinSCANOPY analysed image with percent canopy closure.

Table 1 depicts the calculated canopy closure percentage of each plot calculated by the winSCANOPY program after classification in eCognition. It also shows the summary of the flight accuracy assessments run in ArcGIS after classification in eCognition. In the summary table, the traditional, pixel-based classifications are shown as well as lichen classification accuracy overall scores. It displays the ascending accuracies of each plot image with the respective canopy closure (%), where the relationship between canopy closure and accuracy may be seen. An average image classification accuracy of 68% was observed, while an average of 57% accuracy was documented for lichen classification. Flight 242 returned the highest classification accuracy at 86%, also having the highest canopy closure percentage at 88%. Furthermore, the lowest classification accuracy was returned from plot 223, with a correspondingly low canopy closure percentage. Therefore, if seeking a classification accuracy above or equal to 80%, one should avoid stands with less than 77% canopy closure. However, if the goal is to only use sites that may classify lichen with greater than 80% classification accuracy, then one should use sites with less than or equal to 88% canopy closure.

Table 1. Accuracy of image classification (%) with corresponding canopy closure (%) for each plot.

Plot	Canopy Closure (%)	Pixel-based Accuracy of Entire Image (%)	Lichen Classification Accuracy (%)
242	88	86	82
568	77	80	62
220	39	56	68
268	66	71	58
267	49	66	59
464	39	64	40
223	6	56	30

Source: ArcGIS and WinSCANOPY 2018

The reduced classification accuracy associated with looking at lichen classification alone is indicative of the effect of classifying other factors in each image. For example, plot 568 had exceptional accuracy in classifying shadows, driving up the overall classification accuracy, however bare ground was wrongly classified as lichen often, leading to the lower lichen classification accuracy. It is also important to note that the reduced overall accuracy of plot 220 was due to shadow being classified as vegetation, which does not affect results if solely concerned with lichen classification accuracy.

DISCUSSION

The aim of the study has been to assess the effects of forest canopy closure on the accuracy of UAV imagery classification using eCognition and winSCANOPY software. Under a canopy, the understory layers are in direct light, shade, or become submerged in shadow depending on camera angle. In optical remote sensing the understory reflectance may mix with the overstory, leading to complications in image interpretation and classification (Korpela 2008). Identifying the amount of canopy closure that impedes classification accuracy in lichen detection is therefore crucial if wanting to apply these remote sensing lichen detection techniques to management programs (Rautiainenetal et al. 2007). An evaluation of the effects of canopy cover on the seven selected sites were analysed, however further study with more variable canopy cover is required. The number of samples used in the study are too few to make an accurate statistical analysis based on literature by Hogg and Tanis (2005), stating a sample size greater than 25 to 30 samples is required to run a statistical analysis. Nevertheless, classification of lichen species and its relationship to canopy cover are rare, therefore the results of this study constitute a preliminary assessment on this topic, contributing further knowledge to the subject.

Typically, an overall accuracy score of 75% is ideal (ARSET 2018) for image classification. This is easier with coarse imagery than it is with very high-resolution imagery, as there is a significant growth of detail and information. Increasing the number of classes as part of the classification process increases the potential for error and lowers the overall score with 4-band imagery. To mitigate this source of error, only four classes were used. These included a lichen class, not lichen class, shadow class, and vegetation class. This was to ensure accuracy was based on the correct classification of lichen rather than vegetation or shadow. An assessment of lichen classification alone was also computed, to better represent the effects of canopy closure on lichen detection specifically.

Overall, forest vegetation was classified consistently while lichen was difficult to separate from other landcover types. This is thought to be due to the strong shadows that cover the ground and lichen (Solheim et al. 2000). Another contributing feature is the time of image collection, being mid-summer, the peak of vegetation cover. The classifications heavily rely on reflectance values, leading to lower classification accuracies because the algorithms have trouble distinguishing between rocks and lichen (Rapalee et al. 2001). This was alleviated by using an additional DEM layer, leading to height values combined with reflectance values, increasing accuracy in each custom rule set. In the future, lichen surveys conducted soon after snow melt, during leaf-off season, could help to improve these shortcomings.

The addition of a DEM layer to the classified images was an addition which attempted to aid in the delineation between vegetation, bare ground, and lichen, all of which were difficult to accurately classify based on spectral characteristics. Studies have found that the addition of this layer into the classification scheme has the potential to improve accuracy (Franklin et al. 1991; Franklin 1994; Li and Chen 2005; Nagendra 2001), which was further exemplified by this study. It was found, during the classification process, that the addition of a DEM layer greatly improves accuracy of classifications, allowing the distinction between other features and lichen when shadows and shade impedes this process. Vegetation and lichen, especially the shrub layer within stands, posed a major challenge for classification. Most custom rule sets were based around the DEM layer, allowing a quick and simple delineation between the lichen and shrubs and surrounding trees. A shortcoming of the use of this layer exists with delineating bare ground from the lichen layer. It was found that although the DEM layer aided significantly in reducing misclassification with vegetation, the bare ground and rock features were highly misclassified. This resulted in better classifications under higher canopy closure, as lichen classification was based on trees and lichen. It is suggested that a more detailed DEM layer, with better coverage, would be applied in the future. This is due to the constraint experienced with the DEM layer used for the purpose of this study, which was not accurate enough to distinguish lichen from the bare ground under the canopy.

Reindeer lichen are lighter colored, reflecting more light in blue to yellow wavelengths when compared to green vegetation (Nelson et al. 2013). Although no study has focused on the continuous mapping of usnic lichen, it has been discussed that this substance is in most lichen that caribou eat, having a pale-yellow pigment. This renders the lichen spectrally distinct which is a useful characteristic in remote sensing (Peltoniemi et al. 2005; Nelson et al. 2013). This was utilized in rules made extracting the green band in the UAV imagery classification. The research also suggests additional rules focused on these spectral characteristics could improve accuracy, especially in the delineation of vegetation and lichen, which were difficult to accurately classify. Due to the findings by Nelson et al. (2013) the NIR layer was extensively used during rule set classification. It has been concluded that dark lichens absorb electromagnetic spectrums, but their reflectance is distinct in the NIR band (Nelson et al. 2013), correlating to the increased classification accuracy when utilizing this layer. Although these bands did ensure adequate classification of the UAV imagery, increased accuracy was achieved when other feature classes and layers were utilized in conjunction with this.

The result of this study supports my hypothesis in that canopy openness will affect lichen classification accuracy, however not in the way that was previously thought. It was postulated that as canopy closure increased, classification accuracy would correspondingly decrease. It was found however, that as canopy closure increases, classification accuracy increases. Overall, the classification accuracy was below an applicable accuracy for management uses, however, the knowledge gained from this study demonstrates the point at which canopy closure becomes a factor in lichen classification accuracy. The knowledge gained from this study may be applied in the future for mapping of lichen, potentially for the NCASI Caribou project, where the universal ruleset may be applied. However, the information gathered from this study suggests that UAV image classification for lichen detection should be reserved for stands with more than 77% canopy closure, as the accuracy of assessments significantly decreases after this point.

Although the classification accuracies observed in this study are correlated to the percent canopy closure, it may be extrapolated that bare ground spectral signatures play a more significant role in misclassification. Ground surfaces and understory components contribute to spectral variation (Nagendra 2010). Therefore, the reduced accuracy associated with canopy openness is directly associated to the bare ground and rock found throughout open sites. The light colouration of these features make classification by both computer software and human interpretation limited as there is difficulty in identification. The DEM layer used in abundance throughout this study aided significantly with these limitations, however the accuracy of the DEM was insufficient in delineating the difference in inches that was experienced between lichen and bare ground.

During the data collection period, time was restricted where rain and wind played a major role (Wilkie 2018). The resulting image collection occurred on days with full sun or slight cloud. Image collection in full sun results in images with high amounts of shadows. Combining this with the change in sun angles between flights, shadows caused a major processing issue, post-flight. Shadows mean reduced information picked up by the camera in those areas, resulting in wrong or no classifications (Solheim et al. 2000). In open areas a trees shadow may extend over several feet, leading to misinterpretation, whereas in a closed canopy the shadow is interrupted by surrounding trees. This source of error may have played a role in the increased classification accuracy experienced under greater canopy closure. This was managed by creating a shadow feature class and classifying those areas as such, however identification of shadows and classifying them accurately was a challenge. Ideally, UAV imagery would be collected on overcast days which would minimize the presence of shadows and reduce high levels of contrast between features like rock, aggregates, coarse woody debris, and lichen.

The winSCANOPY software used in this study was a version suited to black and white images, where an updated version could process colour images. In lieu of this, the colour images collected using the winSCANOPY unit in the field had to be classified in eCognition where two classes, one being tree, one being sky, was used. This may have affected the results tabulated in winSCANOPY as the classified images were saved as screen grabs, subjected to pixilation and misclassification during this process.

The universal rule set developed for the purpose of this study was applied across all sites. This was done to ensure it could be applied broadly across different forests stands, where the rule set was applied on known locations that can later be applied to new, unknown areas to classify the forest cover. However, to improve accuracy on each image, unique rule sets were created. This reduced the applicability of results for future, however, increased the accuracy of each classification to ensure the correlation between canopy closure and UAV imagery collection could be identified.

The lighting conditions for various sites were different, based on weather conditions. Therefore, the image stacking process struggled to align the RGB and NIR bands. This could be an artifact of the lighting conditions or that Agisoft didn't create the ortho-imagery equally (Wilkie 2018). Unfortunately, there was no way to colour correct all the imagery together to have the same values with changing sun angles. The best way to avoid these problems is to have a larger image acquisition window and fly with better lighting conditions. Otherwise, some features that are the same between different photos, flight heights and sites may look different and so be classed as different.

Each classified image was approximately 0.5 ha, where photos collected for winSCANOPY were collected in the center of the plot. Therefore, a limited amount of the stand was accounted for in the analysed photographs. It is recommended in future to take multiple canopy closure photos, either randomly throughout the plot or through a systematic graphing system. Currently, the canopy closure percentages tabulated are representative of a very small portion of the stand which were classified. An average of various canopy closure percentages throughout each stand should be recorded and used for future studies to allow for representativeness and accuracy.

It is recommended that further time be spent on classification of non-lichen classes, as this oversight may have reduced accuracy on the overall image classification.

This is exemplified for plot 220, returning much higher accuracies for lichen classification compared to overall image classification. Additionally, for future studies it is recommended that imagery should be collected during “leaf-off” seasons. While this may not affect accuracy in dense conifer stands such as young jack pine sites, it would otherwise. Imagery taken in these seasons would result in less interference between the ground and the sensor. It was also noted that in some areas, varying vertical layers of vegetation above the lichen beds being mapped, blocked all sight of the lichen and prevented image capture. Mapping during leaf-off would remove all deciduous vegetation and allow optical sensors to see further down into the forest cover. It should be noted that most lichen mapping occurs in coniferous stands where caribou overwinter (Korpela 2008; Nordberg and Allard 2014; Peltoniemi et al. 2005; Rautiainen et al. 2007). Therefore, the time of year imagery is collected in Boreal coniferous dominated stands would not greatly affect classification accuracy. Another modification outside of controlling environmental factors includes using a bigger sensor, or a multispectral camera. The NIR camera used had trouble even at 40 meters separating the lichen based on reflectance values alone (Wilkie 2018). A multi-spectral camera could potentially capture narrower spectral bands that would differentiate lichen from the surrounding vegetation. Classification accuracies could be increased in the future given the understandings gained from this project, which could then potentially be applied to the larger portions of the NCASI Caribou project.

CONCLUSION

The conclusion, that at under 77% canopy closure accuracy is affected, supports the finding that canopy closure is directly correlated to the classification efficiency of UAV imagery. Therefore, the findings of this study can contribute to the ongoing analysis of lichen detection for management purposes. However, further investigation to better understand the limits of using UAVs to map lichen is required. The controversies within this field surround the technology used for lichen detection as well as the accuracy and precision each one offers ((Faldorf et al. 2014; Theau and Deguay 2004; Faldoff et al. 2013; Theau and Duguay 2004; Nordberg and Allard 2002; Korpela 2008; Waser et al. 2007). WinSCANOPY technology was found useful in determining the range of percent canopy-closure under which lichen detection is possible. An average classification accuracy of 68% was recorded using UAV imagery with NIR, RGB, and DEM layers, proving effective but limited in its application. This classification method can be applied for management purposes when canopy closure is low enough to allow for accurate classifications. This study falls within the Boreal forest biome, therefore, the results obtained herein over the entire area make this methodology very stable and illustrate its potential application over various land covers.

LITERATURE CITED

[ARSET] Applied Remote Sensing Training. 2018. Accuracy Assessment of land cover classification. NASA. Online Webinar Training. <https://arset.gsfc.nasa.gov/land/webinars/18adv-land-classification>.

Arseneault, D., N. Villeneauve, C. Boismenu, Y. Leblanc, and J. Deshaye. 1997. Estimating lichen biomass and caribou grazing on the wintering grounds of northern Quebec: An application of fire history and landsat data. Journal of Applied Ecology, 34(1), 65-78.

Casanova, P., M. Black, P. Fretwell, and P. Convey. 2015. Mapping lichen distribution on the Antarctic Peninsula using remote sensing, lichen spectra and photographic documentation by citizen scientists. Polar Research, 34(1).

Colpaert, A, J. Kumpula, and M. Nieminen. 1995. Remote sensing, a tool for reindeer land management. Polar Record, 31, 235-244.

Falldorf, T., O. Strand, M. Panzacchi, and H. Tommervik. 2014. Estimating lichen volume and reindeer winter pasture quality from Landsat imagery. Remote Sensing of Environment, 140, 573-579.

Franklin, S. E., C. F. Blodgett, S. Mah, and C. Wrightson. 1991. Sensitivity of CASI data to anisotropic reflectance, terrain aspect and deciduous forest species. Canadian Journal of Remote Sensing, 17, 314-321.

Franklin, S. E. 1994, Discrimination of subalpine forest species and canopy density using digital CASI, SPOT PLA, and Landsat TM data. Photogrammetric Engineering and Remote Sensing, 60, 1233–1241.

Gilichinsky, M., P. Sandstrom, H. Reese, S. Kivinen, J. Moen, and M. Nilsson. 2011. Mapping ground lichens using forest inventory and optical satellite data. International journal of remote sensing, 32(2), 455-472.

Hogg, R. and E. Tanis. 2005. Probability and statistical inference. Pearson Library of Congress, 7, 552 pp.

Jarcuska, B., S. Kucbel, and P. Jaloviar. 2010. Comparison of output results from two programmes for hemispherical image analysis: Gap Light Analyser and WinScanopy. Journal of Forest Science, 56 (4), 147-153.

Jiang, Z., A. Huete, T. Miura, and K. Didan. 2008. Development of a two-band enhanced vegetation index without a blue band. Remote Sensing of Environment, 112(10), 3833-3845.

Korpela, I. 2008. Mapping of understory lichens with airborne discrete-return LiDAR data. Remote sensing of environment. 112(10), 3891-3897.

Li, J. and W. Chen. 2005. A rule-based method for mapping Canada's wetlands using optical, radar, and DEM data. International Journal of Remote Sensing, 26(2), 5051-5069.

Murray, B. 2013. Spatial and temporal patterns in ungulate-ecosystem interactions. Dissertation, Michigan Technological University, 123.

Nagendra, H. 2001. Using remote sensing to assess biodiversity. International Journal of Remote Sensing, 22(12), 2377-2400.

Nelson, P., C. Roland, M. Macander, and B. McCune. 2013. Detecting continuous lichen abundance for mapping winter caribou forage at landscape spatial scales. Remote sensing of environment. 137, 43-54.

Nordberg, M.L., A. Allard. 2014. A remote sensing methodology for monitoring lichen cover. Canadian Journal of Remote Sensing, 28 (2), 262-274.

Peltoniemi, J., S. Kaasalainen, J. Naranen, M. Rautiainen, P. Stenberg, H. Smolander, S. Smolander, and P. Voipio. 2005. BRDF measurement of understory vegetation in pine forests: dwarf shrubs, lichen, and moss. Remote Sensing of Environment, 94, 343-354.

Petzold, D. E. and S. N. Goward. 1988. Refelctance spectra of subarctic lichens. Remote Sensing of Environment, 24, 481-492.

Rapalee, G., L. Steyaert, and F.G. Hall. 2001. Moss and lichen cover mapping at local and regional scales in the boreal forest ecosystem of central Canada. Journal of Geophysical Research, 106, 33551-33563.

Rautiainen, M., J. Suomalainen, M. Mottus, P. Stenberg, P. Voipio, J. Peltonienmi, et al. 2007. Coupling forest canopy and understory reflectance in the Arctic latitudes of Finland. Remote sensing of environment, 94, 343-354.

Rees, W. G., O. V. Tutubalina, and E. I. Golubeva. 2004. Reflectance spectra of subarctic lichens between 400 and 2400 nm. Remote Sensing of Environment, 90, 281-292.

Rees, W. G., M. Williams, and P. Vitebsky. 2003. Mapping land cover change in a reindeer herding area of the Russian Arctic using Landsat TM and ETM+ imagery and indigenous knowledge. Remote Sensing of Environment, 85, 441-452.

Solheim, I., O. Engelsen, B. Hosgood, and G. Andreoli. 2000. Measurement and modelling of the spectral and directional reflection properties of lichen and moss canopies. Remote Sensing of Environment, 72, 78-94.

Theau, J. and C. R. Duguay. 2004. Lichen mapping in the summer range of the George River caribou herd using Landsat TM imagery. Canadian Journal of Remote Sensing, 30(6), 867-881.

Theau, J. and C. R. Duguay. 2005. Mapping lichen in a caribou habitat of Northern Quebec, Canada, using enhancement classification method and spectral mixture analysis. Remote sensing of environment, 94(2), 232-243.

Waser, L., M. Kuechler, M. Schwarz, E. Ivits, and S. Stofer. 2007. Prediction of lichen diversity in an UNESCO biosphere reserve – correlation of high resolution remote sensing data with field samples. Environmental modelling and assessment, 12(4), 315-328.

Waser, L., S. Stofer, M. Schwartz, M. Kuchler, E. Ivits, and C. Scheidegger. 2005. Prediction of biodiversity – regression of lichen species richness on remote sensing data. Community Ecology, 5(1).

Wilkie, R. 2018. Lichen classification form UAS imagery. LU-CARIS. 29

Xiaoqin, W, W. Miaomiao, W. Shaoqlang, and W. Yundong. 2015. Extraction of vegetation information from visible unmanned aerial vehicle images. China Academic Journal, 31(5), 152-158.

APPENDICES

APPENDIX I

NCASI PLOT INFORMATION

Plot	PEN (plot #)	SBST	Total Lichen Biomass (Kg/ha)	Lichen 'stand' type	Lichen Stand Code
267/268	172	I	2206.8	Dense, continuous lichen mats	1
464	2	III	1756.5	Lichen/rock outcrop mosaic	3
220	114	I	1027.51	Open forest/lichen intermixes	4
568	57	III	981.92	Unsure (2 or 4)	2/4
242	146	III	714.83	Dense, continuous lichen mats	2
246	150	III	553.51	Lichen/rock outcrop mosaic	3
223	118	I	199.86	Open forest/lichen intermixes	4

APPENDIX II

PLOT 220 RULESET

APPENDIX III

PLOT 223 RULESET

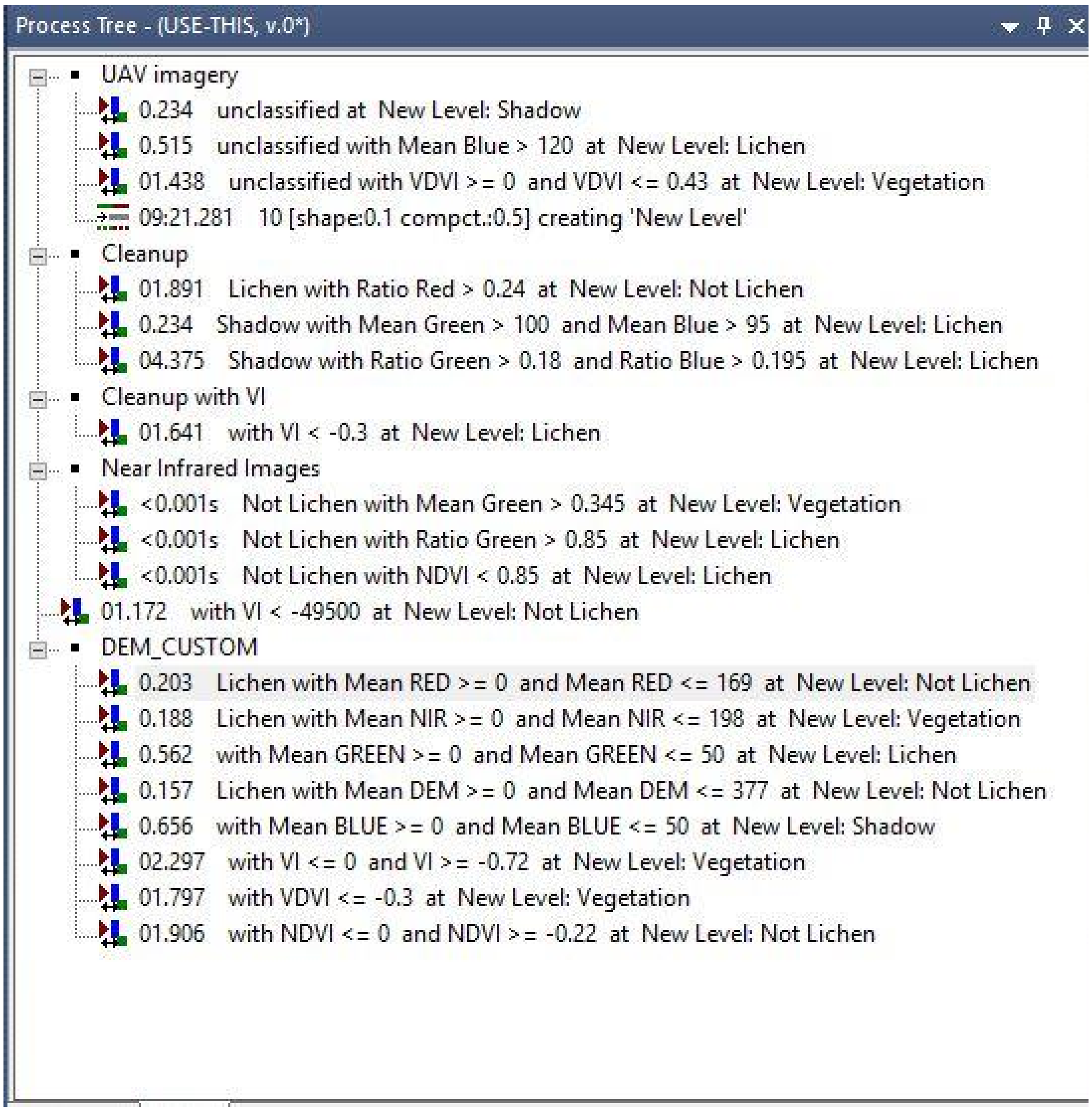

APPENDIX IV

PLOT 242 RULESET

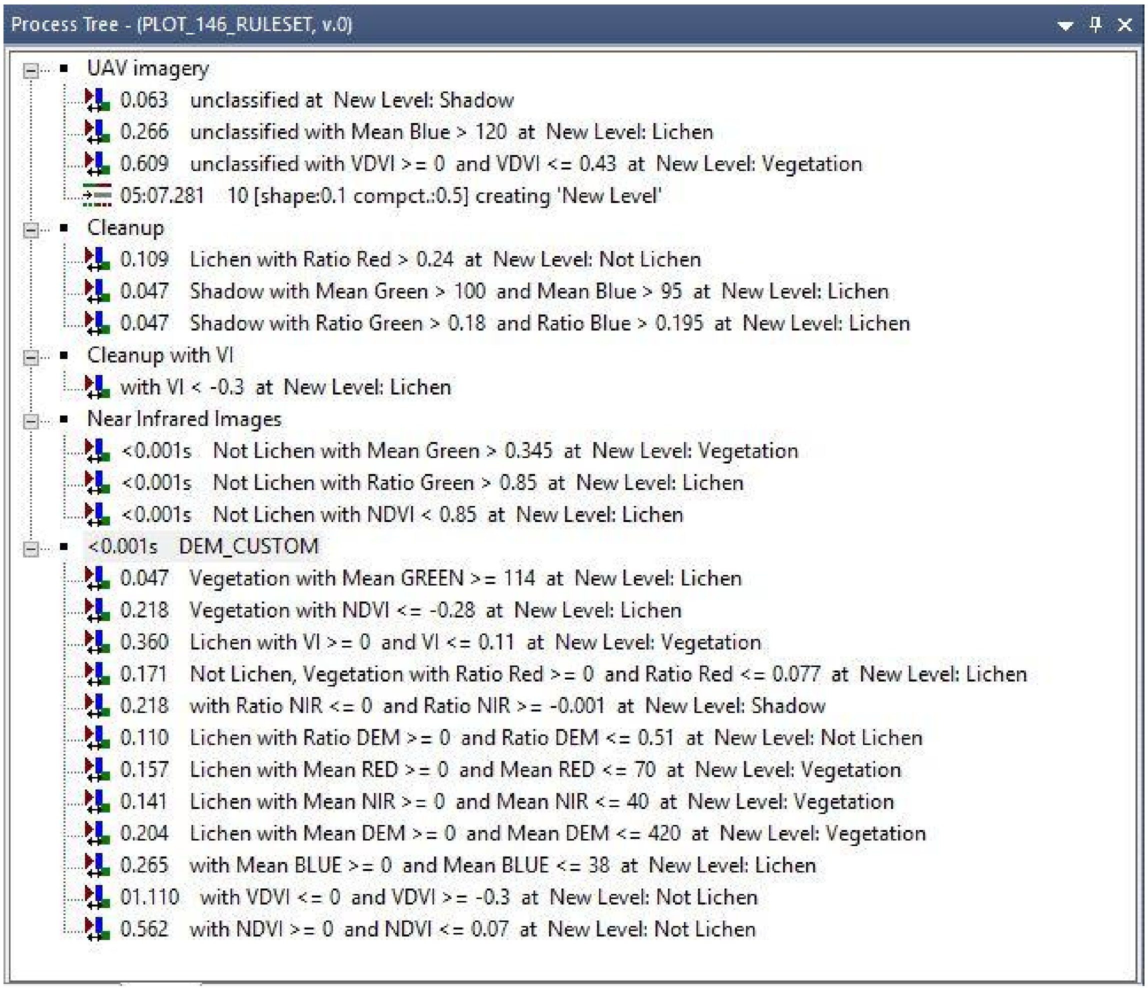

APPENDIX V

PLOT 267 RULESET

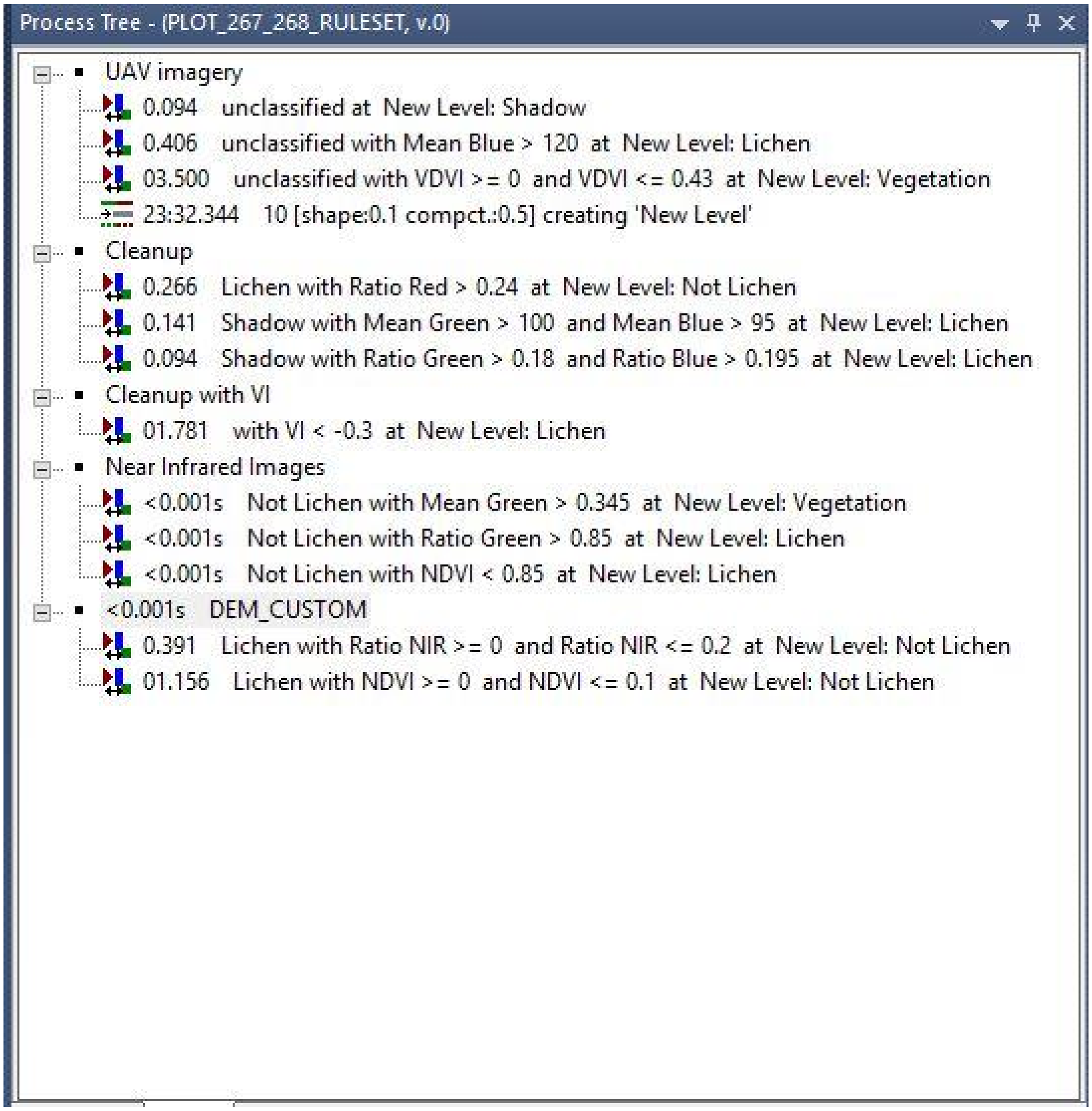

APPENDIX VI

PLOT 464 RULESET

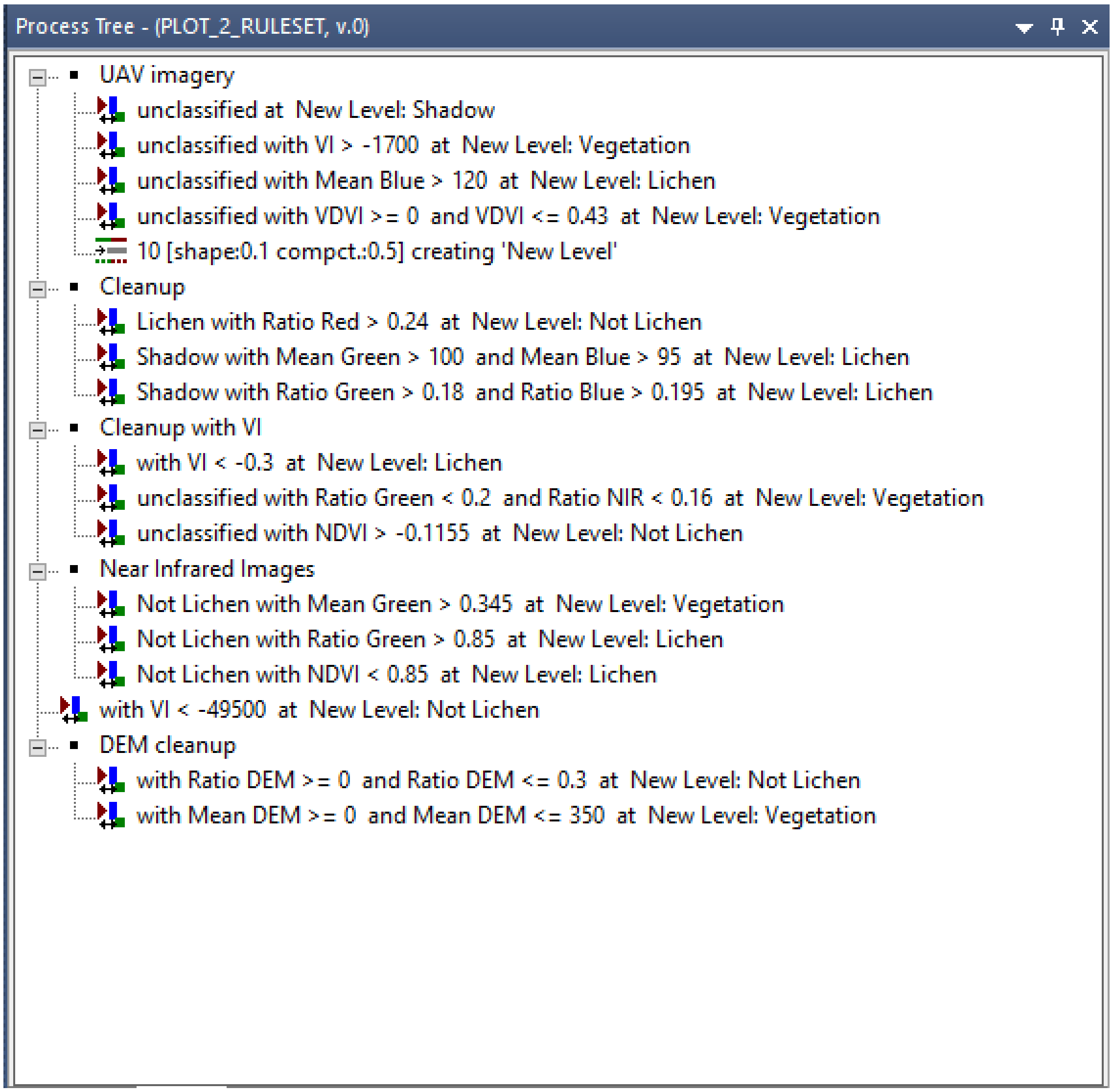

APPENDIX VII

PLOT 568 RULESET

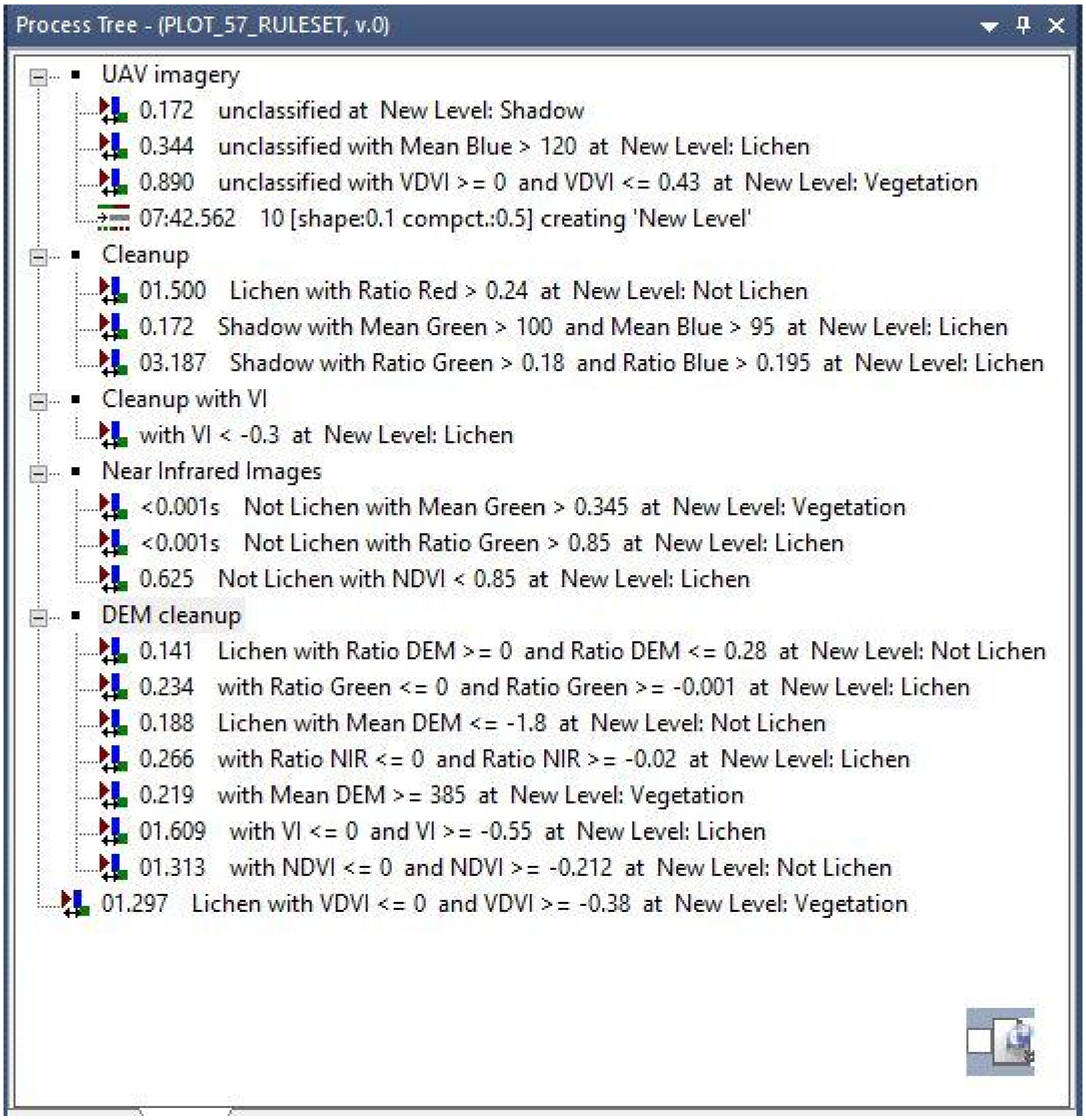

APPENDIX VIII

ACCURACY ASSESSMENT RAW DATA – PLOTS 464, 568, 220, AND 223

Point Number	Classification	Real (Plot 2)
1	3	1
2	3	3
3	1	1
4	1	1
5	3	2
6	3	4
7	3	3
8	3	3
9	3	1
10	1	1
11	3	4
12	3	4
13	3	4
14	3	3
15	3	3
16	3	1
17	4	4
18	3	1
19	3	3
20	3	1
21	3	3
22	3	3
23	4	4
24	2	4
25	3	3
26	3	3
27	1	2
28	1	1
29	3	3
30	1	1
31	3	1
32	1	2
33	3	3
34	3	3
35	1	4
36	1	1
37	3	4
38	3	3
39	2	2
40	2	2
41	1	2
42	1	2
43	2	2
44	2	2
45	3	3
46	3	3
47	3	1
48	3	1
49	1	4
50	4	4
51	2	2
52	1	1
53	1	1
54	1	1
55	1	4
56	4	4
57	3	1
58	2	2
59	4	4
60	3	3
61	1	4
62	1	1
63	1	1
64	3	3
65	2	2
66	4	4
67	3	3
68	3	1
69	1	1
70	1	1
71	3	3
72	4	4
73	3	2
74	3	3
75	3	3
76	3	3
77	1	2
78	3	3
79	3	4
80	3	3
81	1	1
82	4	4
83	3	3
84	1	2
85	3	4
86	3	1
87	3	1
88	3	1
89	1	1
90	3	3
91	1	1
92	1	1
93	3	1
94	3	3
95	3	3
96	3	3
97	4	4
98	1	1
99	3	2
100	1	3
Accuracy (all)		63.63636364
ccuracy (lichen)		40

Point	Classification	Real (Plot 57)
1	1	4
2	4	4
3	4	4
4	1	1
5	1	1
6	1	2
7	4	4
8	1	1
9	2	2
10	2	2
11	4	4
12	2	2
13	3	3
14	4	3
15	4	4
16	2	2
17	4	4
18	4	4
19	4	4
20	3	3
21	2	3
22	4	2
23	3	3
24	1	1
25	2	2
26	1	1
27	1	1
28	3	3
29	4	4
30	4	4
31	1	1
32	1	2
33	1	2
34	4	4
35	1	1
36	3	3
37	1	1
38	2	2
39	3	3
40	3	3
41	1	2
42	4	4
43	1	2
44	3	3
45	1	1
46	2	2
47	1	2
48	2	3
49	3	3
50	1	1
51	4	4
52	4	4
53	1	2
54	1	1
55	2	2
56	4	4
57	4	4
58	1	1
59	4	4
60	4	4
61	1	1
62	1	1
63	4	4
64	1	1
65	1	1
66	4	4
67	4	4
68	2	2
69	1	1
70	1	1
71	4	4
72	4	4
73	3	3
74	2	4
75	4	4
76	4	4
77	4	4
78	2	2
79	1	1
80	3	3
81	1	2
82	3	3
83	3	2
84	1	1
85	1	2
86	1	1
87	3	3
88	3	3
89	4	4
90	1	2
91	1	2
92	4	4
93	2	2
94	4	4
95	1	1
96	2	1
97	3	3
98	1	2
99	2	2
100	2	2
Accuracy (all)		80
ccuracy (lichen)		62

Point	Classification	Real
1	2	4
2	2	4
3	1	1
4	2	4
5	3	2
6	3	3
7	2	4
8	3	4
9	1	1
10	3	3
11	3	4
12	2	4
13	3	1
14	3	3
15	1	1
16	2	4
17	3	3
18	3	2
19	3	3
20	3	4
21	2	4
22	3	3
23	1	3
24	3	3
25	3	3
26	3	2
27	1	1
28	1	1
29	3	4
30	2	4
31	1	1
32	1	1
33	2	2
34	1	1
35	3	3
36	3	4
37	1	1
38	3	3
39	2	2
40	3	3
41	1	1
42	3	3
43	1	3
44	1	3
45	1	3
46	1	4
47	3	3
48	1	3
49	3	1
50	1	1
51	2	4
52	3	3
53	3	3
54	1	1
55	3	3
56	3	3
57	3	4
58	3	3
59	3	2
60	3	3
61	3	3
62	3	3
63	3	4
64	1	1
65	3	2
66	2	1
67	3	3
68	3	3
69	3	3
70	3	1
71	3	2
72	1	1
73	3	2
74	1	1
75	1	1
76	1	1
77	1	1
78	3	2
79	3	3
80	3	3
81	3	4
82	3	4
83	3	3
84	1	1
85	3	3
86	2	2
87	1	1
88	3	3
89	3	3
90	2	3
91	3	4
92	3	4
93	3	2
94	3	1
95	3	2
96	3	3
97	3	2
98	3	4
99	1	1
100	1	1
Accuracy (all)		56
ccuracy (lichen)		68

Point	Classification	Real (Plot 118)
1	3	3
2	1	1
3	2	2
4	3	2
5	3	1
6	3	3
7	1	2
8	3	3
9	3	3
10	2	3
11	3	3
12	3	2
13	3	2
14	3	2
15	3	3
16	3	1
17	3	3
18	3	1
19	1	1
20	3	2
21	4	4
22	3	2
23	3	3
24	3	3
25	3	3
26	2	2
27	2	2
28	3	2
29	4	4
30	3	2
31	3	3
32	3	3
33	3	3
34	3	2
35	2	2
36	3	3
37	3	4
38	3	3
39	3	3
40	2	2
41	3	3
42	3	3
43	3	3
44	3	3
45	3	3
46	1	1
47	3	2
48	1	1
49	4	3
50	3	1
51	1	1
52	3	3
53	3	1
54	1	3
55	3	1
56	3	3
57	3	3
58	1	1
59	4	3
60	3	2
61	1	2
62	3	2
63	1	3
64	1	2
65	3	2
66	4	2
67	3	3
68	3	3
69	3	2
70	3	1
71	2	2
72	3	3
73	3	2
74	3	1
75	3	2
76	4	4
77	3	3
78	1	1
79	1	1
80	3	3
81	1	1
82	1	3
83	2	2
84	3	3
85	1	2
86	3	3
87	3	2
88	3	3
89	1	1
90	1	1
91	3	3
92	4	4
93	1	1
94	3	3
95	4	4
96	2	2
97	2	2
98	3	3
99	3	3
100	4	4
Accuracy (all)		51
ccuracy (lichen)		45

APPENDIX IX

ACCURACY ASSESSMENT RAW DATA – PLOTS 242, 267, AND 268

Point	Classification	Real (Plot 146)
1	3	3
2	1	1
3	2	2
4	1	1
5	1	1
6	3	3
7	3	3
8	2	2
9	1	3
10	3	3
11	3	2
12	3	3
13	4	4
14	1	1
15	1	1
16	1	1
17	3	3
18	2	2
19	3	3
20	2	2
21	4	4
22	3	3
23	2	2
24	3	3
25	3	3
26	3	4
27	3	4
28	1	1
29	4	1
30	4	4
31	1	4
32	2	2
33	1	1
34	4	4
35	2	2
36	3	3
37	1	2
38	1	1
39	3	3
40	3	3
41	1	2
42	3	3
43	4	4
44	2	2
45	2	2
46	2	2
47	1	1
48	3	3
49	4	4
50	3	3
51	1	1
52	1	1
53	3	3
54	1	1
55	1	1
56	4	4
57	1	1
58	1	1
59	3	3
60	1	1
61	3	4
62	4	4
63	1	1
64	3	4
65	2	2
66	2	2
67	3	4
68	4	4
69	2	2
70	4	4
71	3	3
72	3	3
73	4	4
74	2	2
75	1	1
76	3	3
77	1	4
78	4	4
79	1	1
80	1	1
81	1	1
82	4	1
83	3	3
84	1	1
85	1	1
86	1	1
87	3	2
88	1	1
89	3	3
90	4	4
91	2	2
92	3	3
93	1	1
94	4	4
95	1	1
96	3	3
97	2	2
98	3	3
99	4	4
100	4	4
Accuracy (all)		86
ccuracy (lichen)		82

Point	Classification	Real (Plot 267)
1	4	3
2	1	4
3	1	1
4	1	1
5	3	3
6	3	3
7	2	2
8	1	1
9	1	2
10	3	3
11	1	1
12	1	2
13	4	4
14	1	4
15	2	2
16	1	1
17	3	3
18	3	3
19	1	2
20	3	3
21	3	3
22	3	3
23	3	4
24	1	2
25	3	3
26	3	3
27	3	3
28	1	1
29	2	2
30	1	1
31	1	2
32	2	2
33	3	4
34	3	2
35	3	3
36	3	2
37	1	1
38	1	1
39	2	2
40	3	3
41	1	1
42	2	2
43	3	3
44	1	2
45	1	1
46	1	1
47	1	4
48	3	3
49	1	1
50	1	2
51	3	4
52	3	2
53	4	4
54	3	4
55	3	3
56	3	4
57	3	4
58	4	4
59	3	3
60	3	3
61	1	4
62	1	4
63	1	1
64	2	2
65	1	1
66	4	4
67	3	3
68	1	1
69	1	1
70	1	2
71	1	1
72	2	2
73	4	4
74	2	2
75	3	3
76	1	1
77	2	2
78	2	2
79	3	3
80	3	4
81	4	4
82	4	2
83	3	1
84	3	3
85	3	3
86	1	3
87	2	4
88	1	4
89	4	4
90	1	1
91	1	1
92	1	1
93	3	4
94	4	2
95	3	3
96	3	1
97	4	2
98	1	1
99	3	2
100	1	1
Accuracy (all)		66
ccuracy (lichen)		59

Point	Classification	Real (Plot 268)
1	3	3
2	1	4
3	1	3
4	1	1
5	3	3
6	3	3
7	2	2
8	1	1
9	1	2
10	3	3
11	1	1
12	1	2
13	4	4
14	1	4
15	2	2
16	1	1
17	3	3
18	3	3
19	1	2
20	3	3
21	3	3
22	3	3
23	3	4
24	1	2
25	3	3
26	3	3
27	3	3
28	1	1
29	2	2
30	1	1
31	1	2
32	2	2
33	3	4
34	3	2
35	3	3
36	3	2
37	1	1
38	1	1
39	2	2
40	3	3
41	1	1
42	2	2
43	3	3
44	1	2
45	1	1
46	1	1
47	1	4
48	3	3
49	1	1
50	1	2
51	3	4
52	3	2
53	4	4
54	3	4
55	3	3
56	3	4
57	3	4
58	4	4
59	3	3
60	3	3
61	1	4
62	1	4
63	1	1
64	2	2
65	1	1
66	4	4
67	3	3
68	1	1
69	1	1
70	1	2
71	1	1
72	2	2
73	4	4
74	2	2
75	3	3
76	1	1
77	2	2
78	2	2
79	3	3
80	3	4
81	4	4
82	2	2
83	3	1
84	3	3
85	3	3
86	1	3
87	4	4
88	1	4
89	4	4
90	1	1
91	1	1
92	1	1
93	3	4
94	2	2
95	3	3
96	3	3
97	2	2
98	1	1
99	3	2
100	1	1
Accuracy (all)		71
ccuracy (lichen)		58

APPENDIX X

IMAGE CLASSIFICATION VALUES

Value	Classification
1	Lichen
2	Not Lichen
3	Vegetation
4	Shadow

APPENDIX XI

CLASSIFIED PLOT IMAGES

PLOT 220

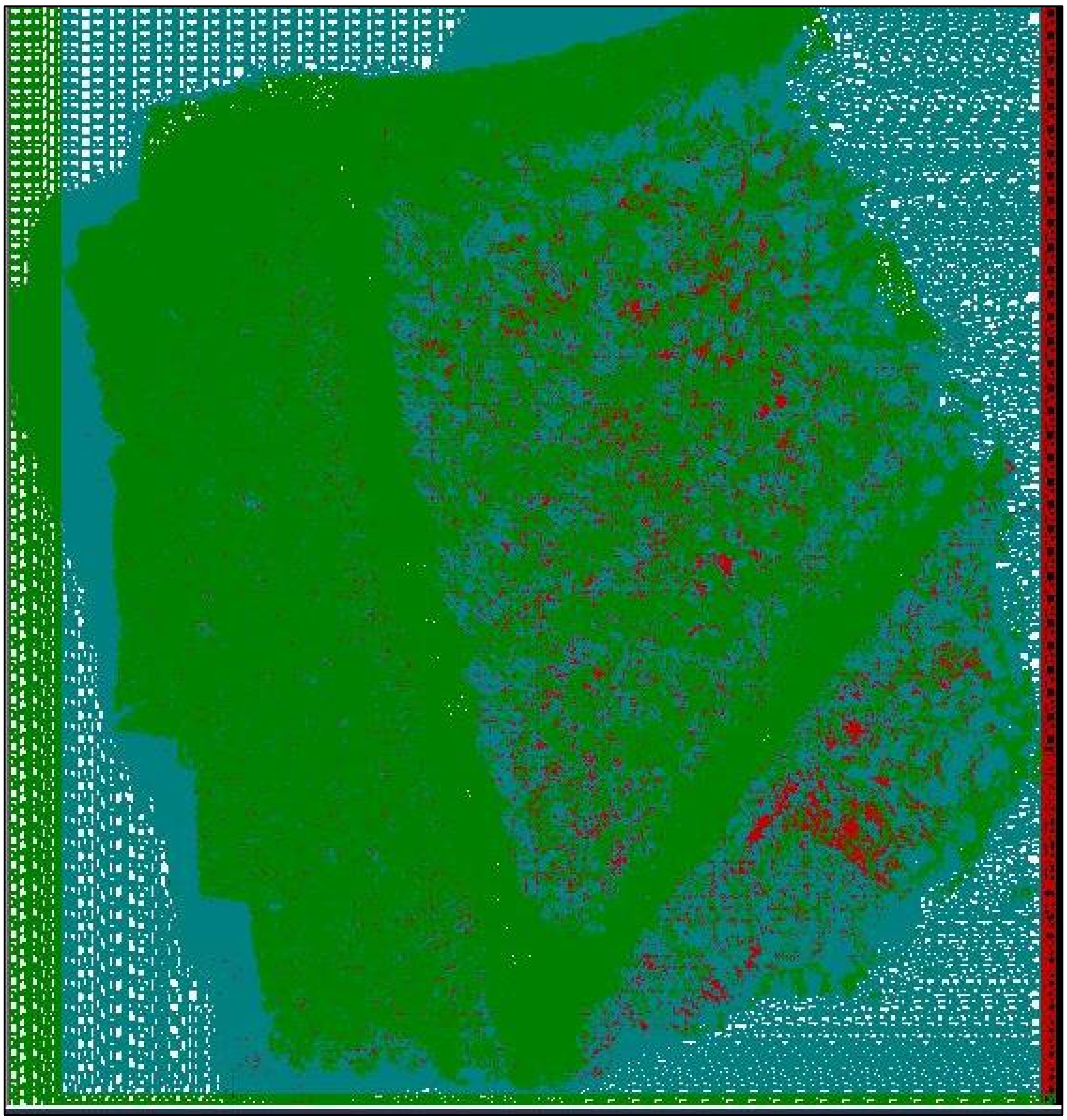

PLOT 568

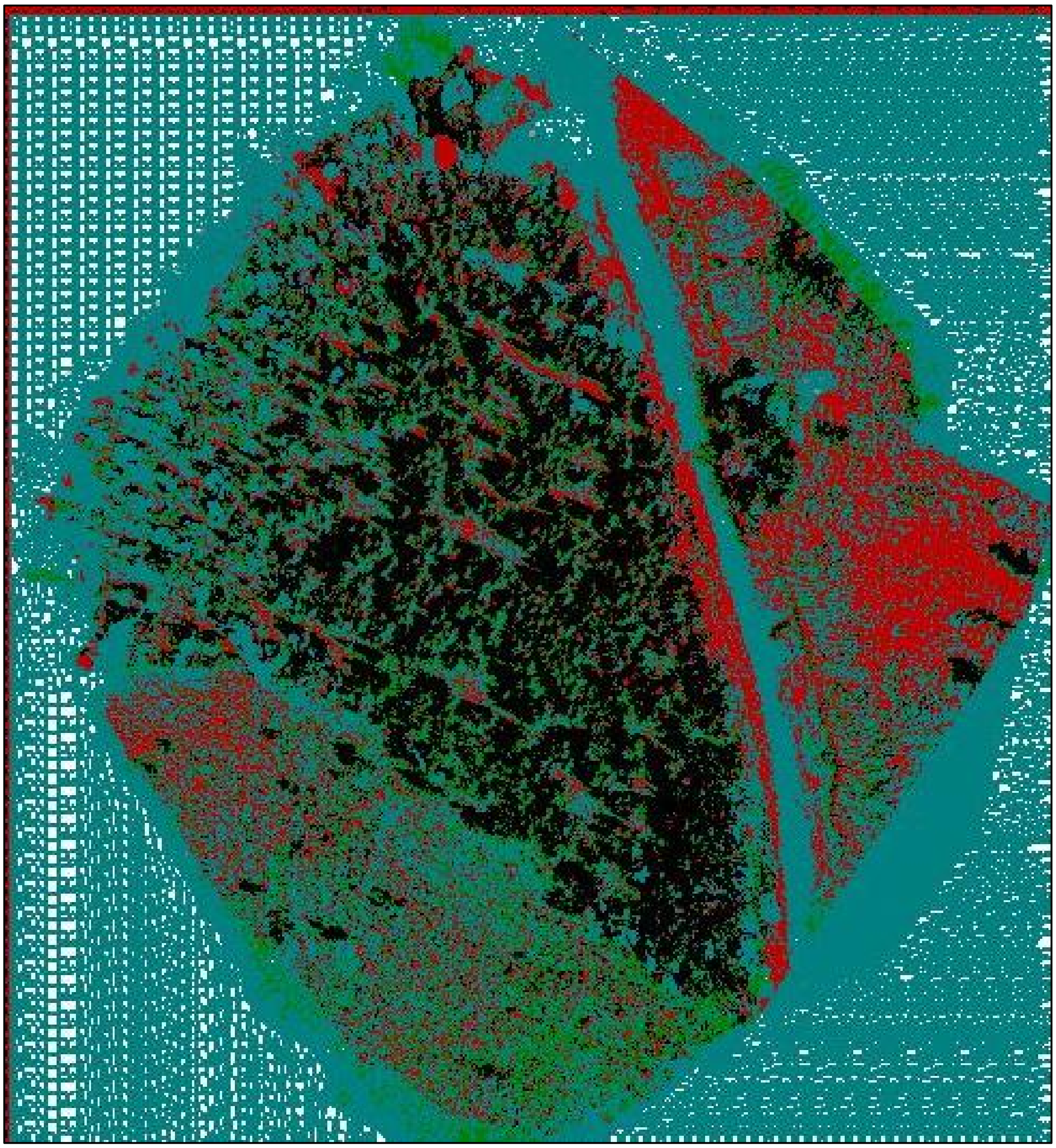

PLOT 464

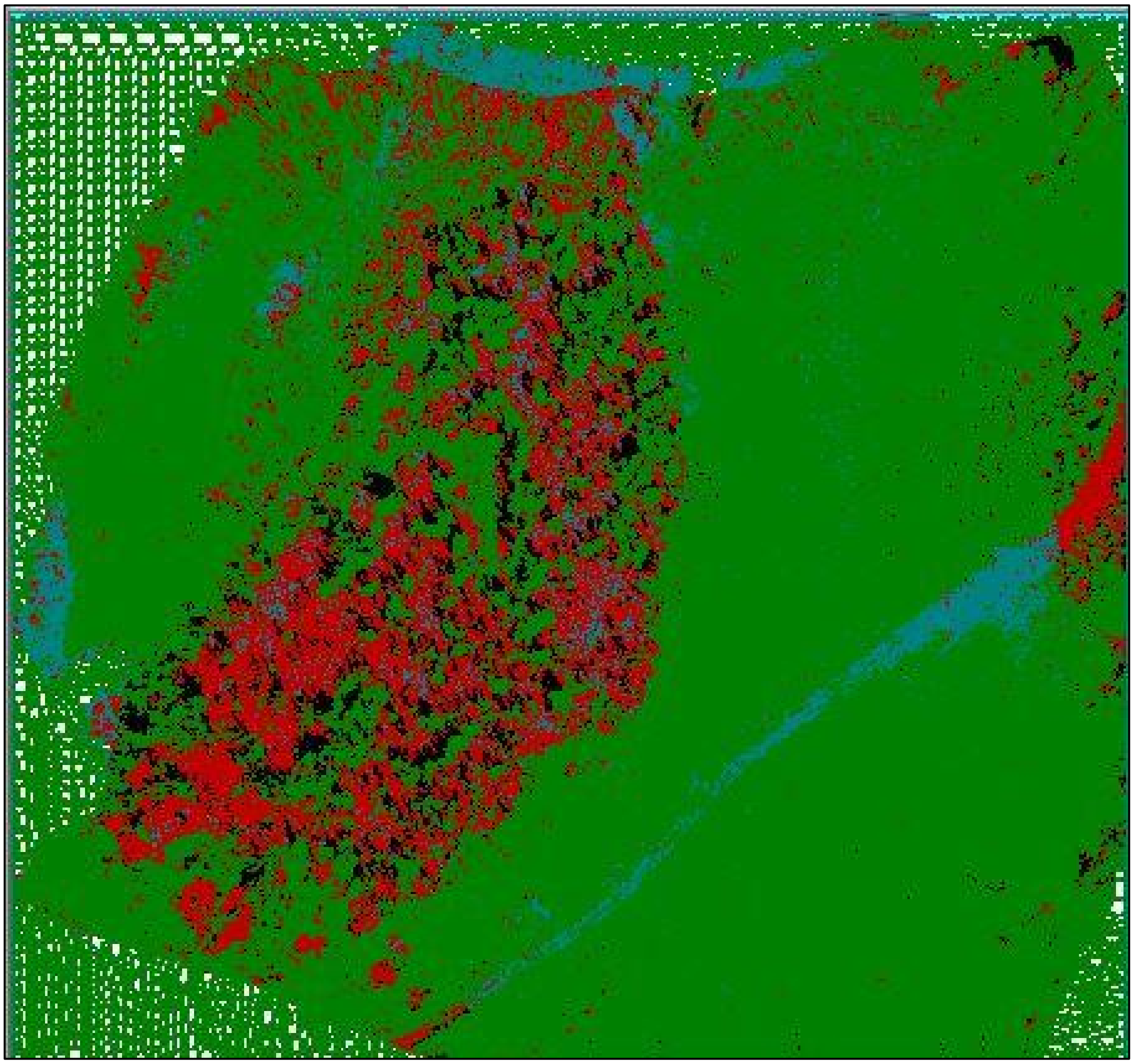

PLOT 267 AND PLOT 268

PLOT 223

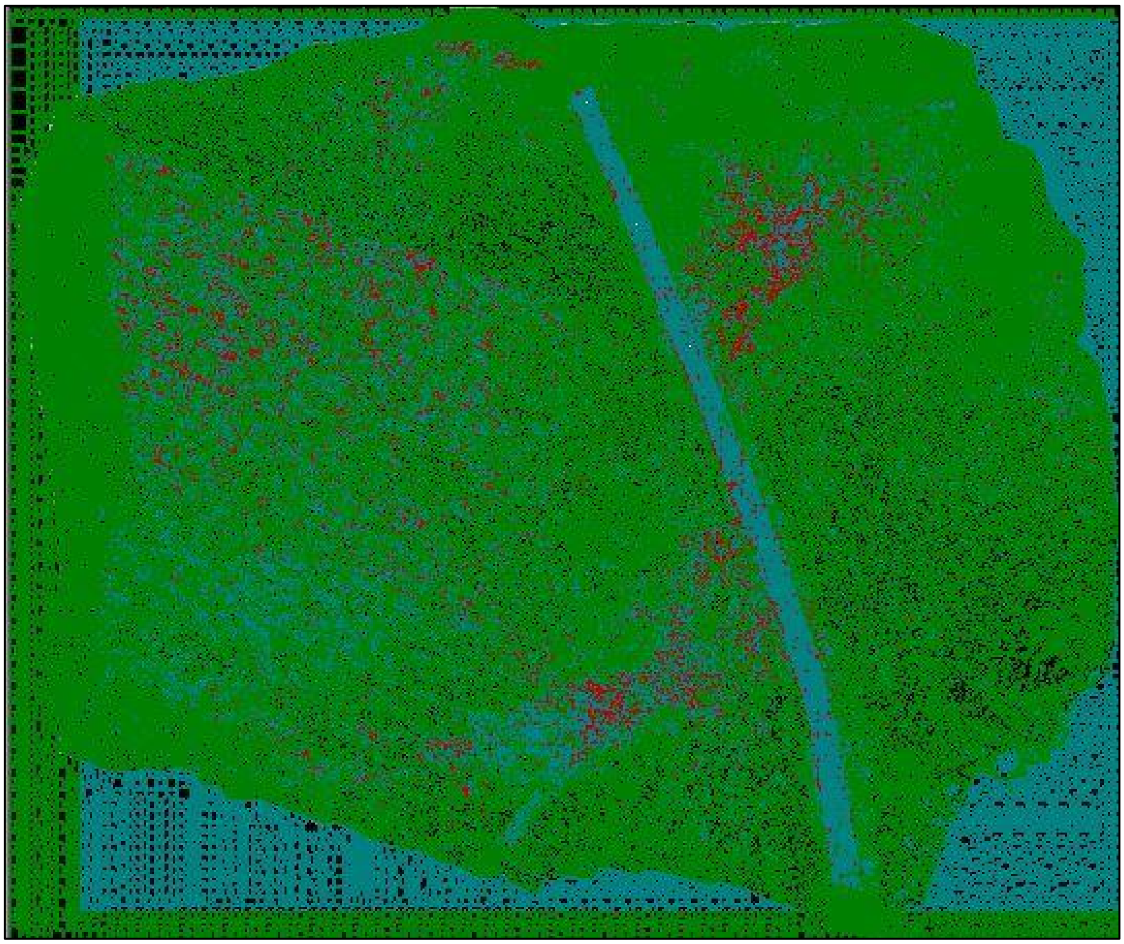

APPENDIX XII

WINSCANOPY ANALYSIS

PLOT 220

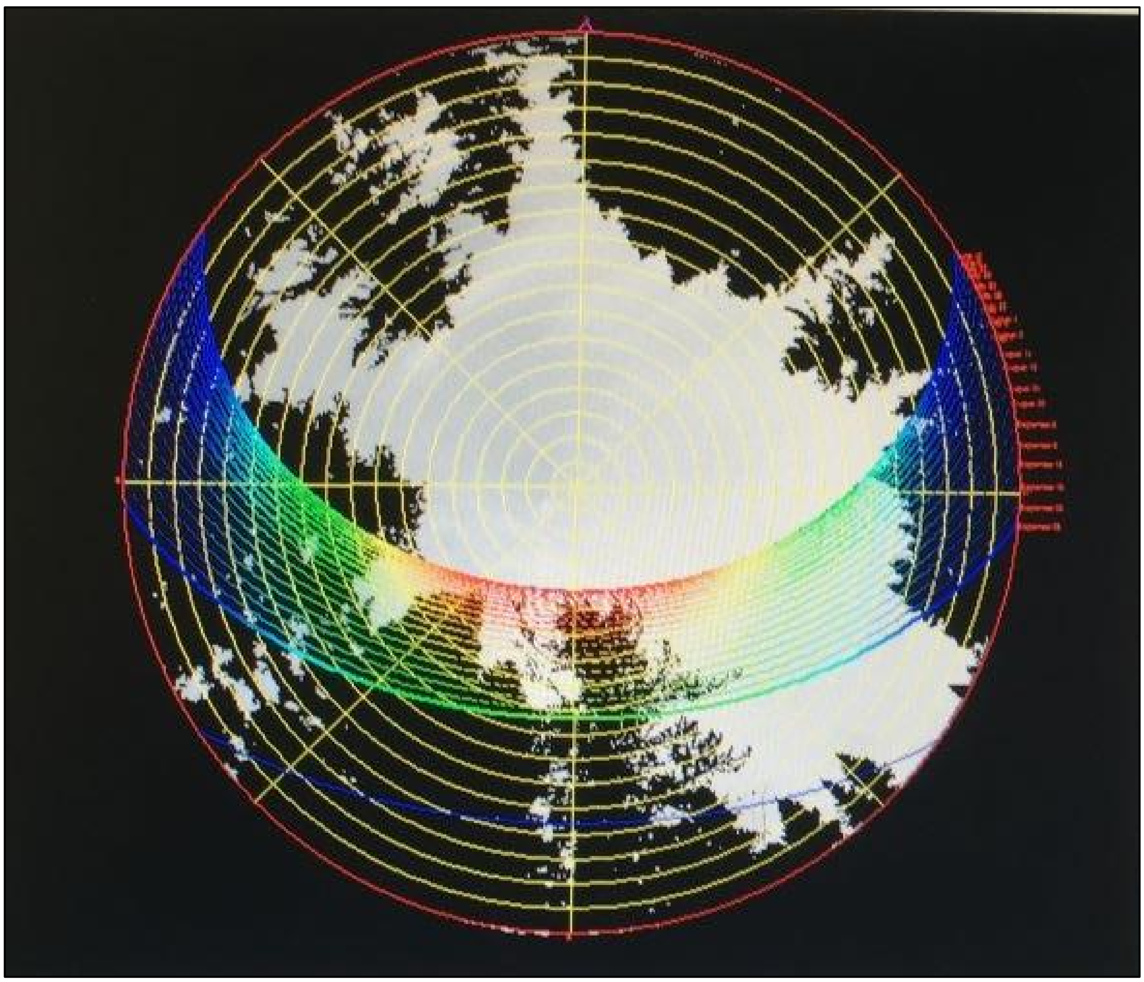

PLOT 568

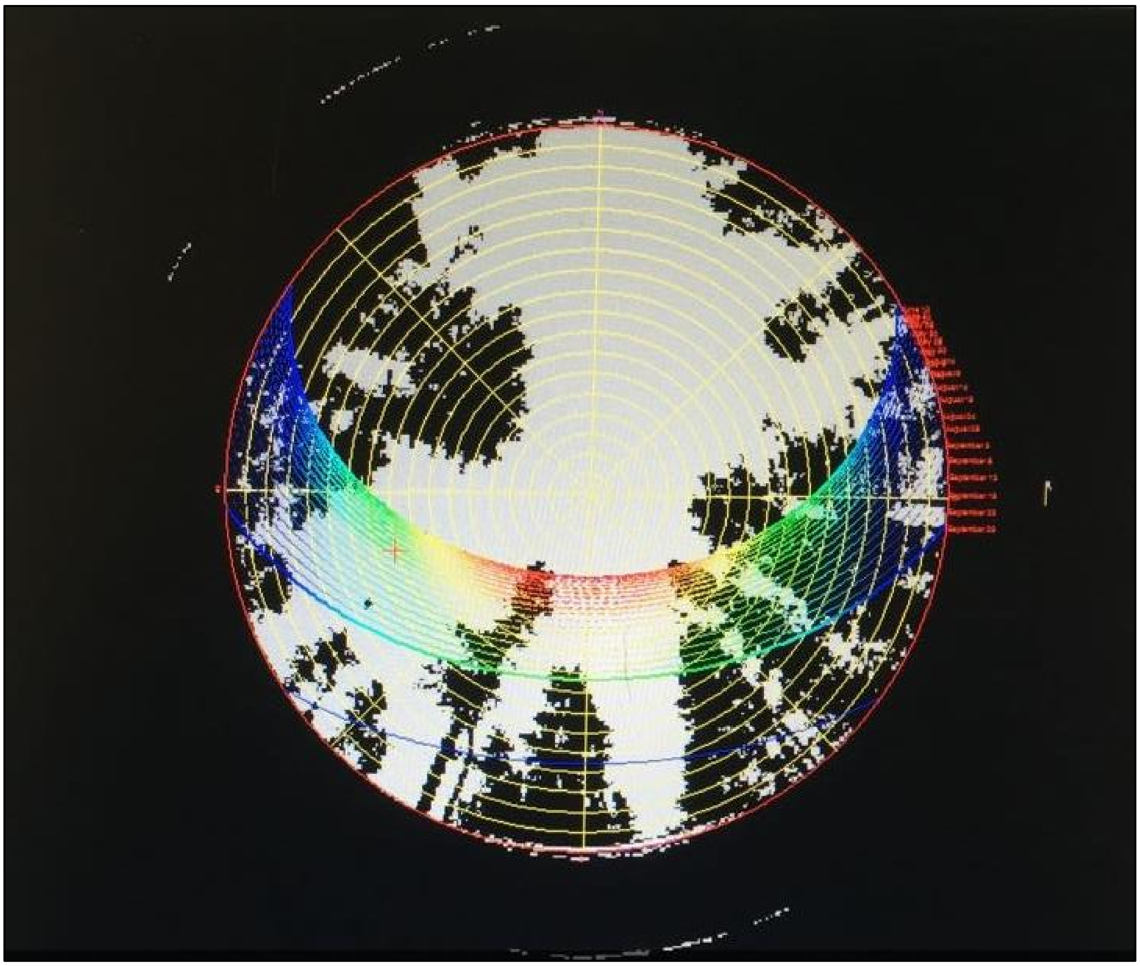

PLOT 464

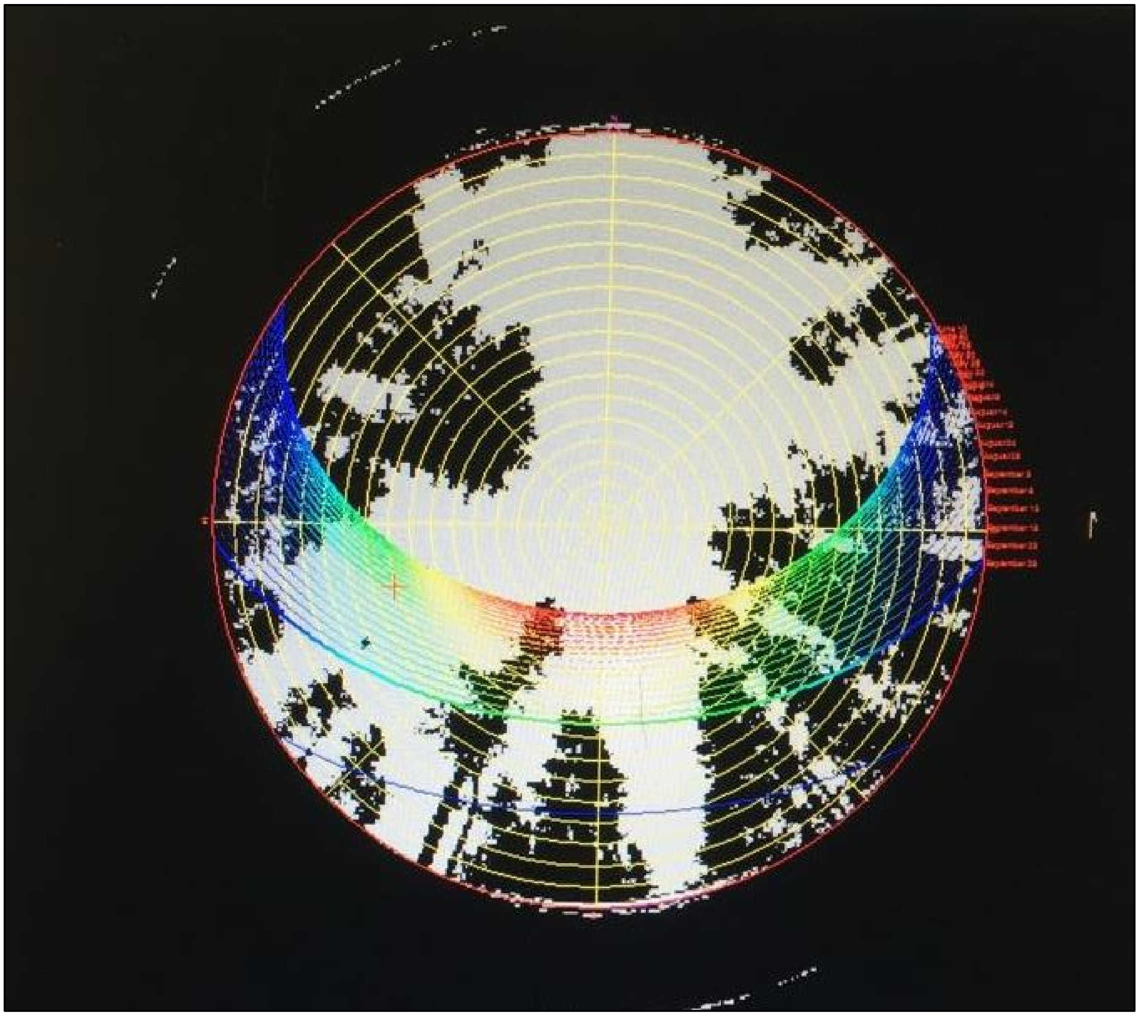

PLOT 268

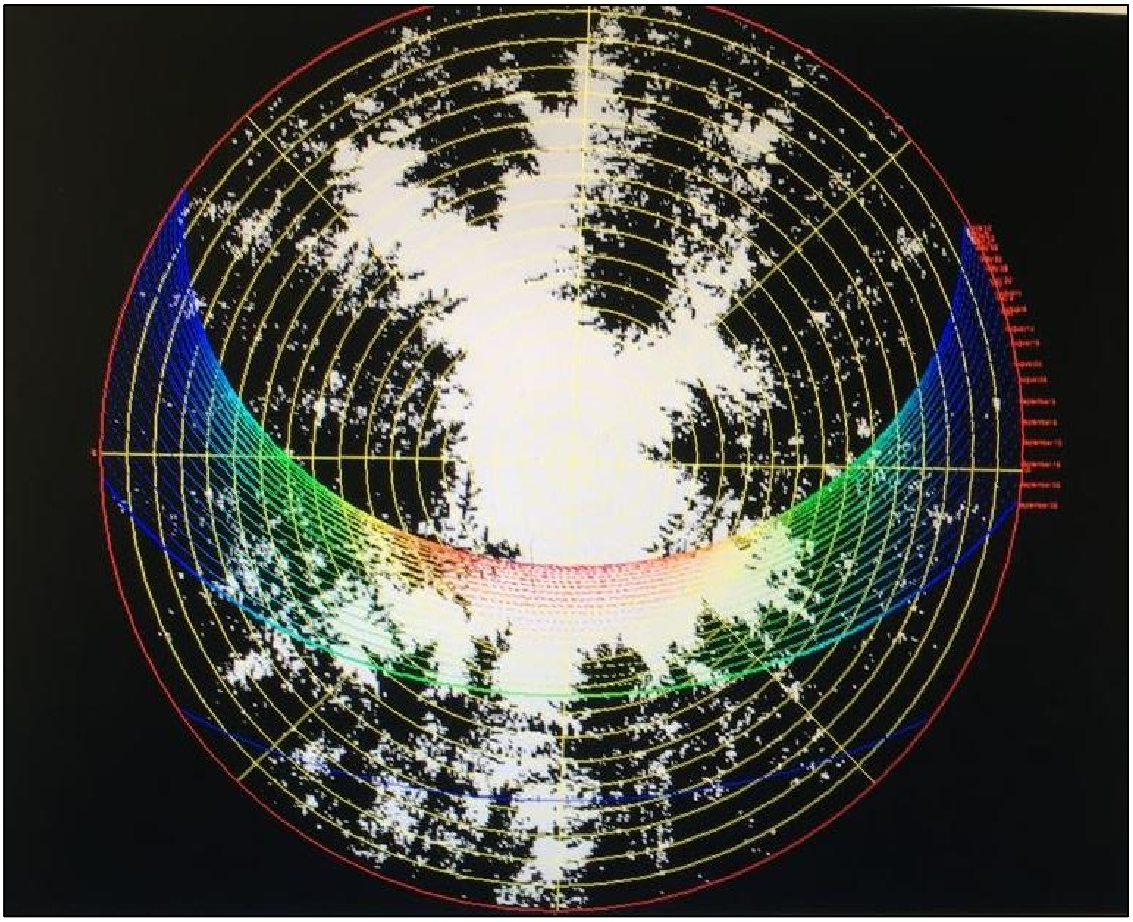

PLOT 242

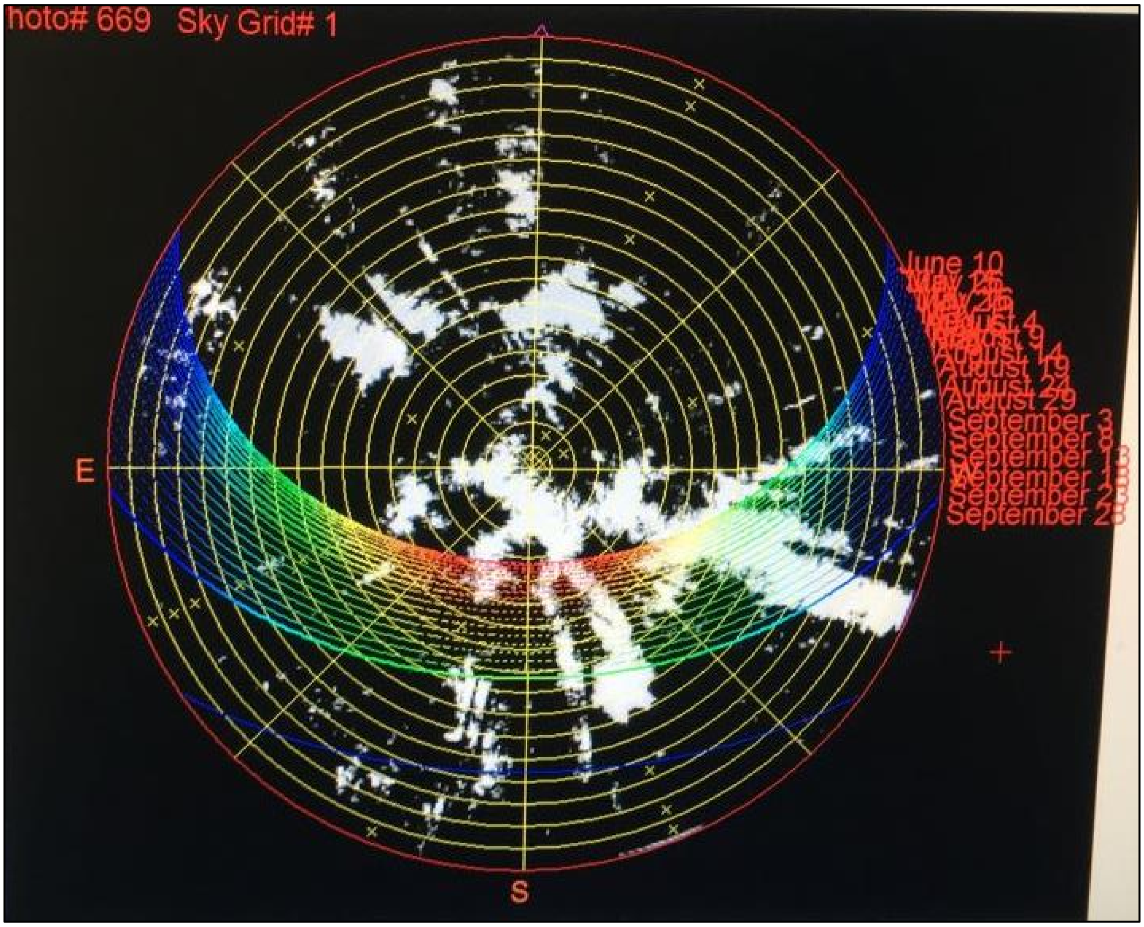
hoto# 669 Sky Grid# 1
E
S
June 10
August 19
August 24
August 29
September 3

PLOT 223